

# CRH Engagement of the Locus Coeruleus Noradrenergic System Mediates Stress-Induced Anxiety

## Highlights

- Inhibition of LC-NE neurons during stress prevents subsequent anxiety-like behavior
- Increased tonic LC-NE neuronal activity promotes anxiety-like and aversive behavior
- CRH<sup>+</sup> CeA-LC projections increase LC-NE activity and promote anxiogenic responses
- CRH<sup>+</sup> CeA-LC-induced anxiety-like behavior is mediated by CRHR1 receptors

## Authors

Jordan G. McCall, Ream Al-Hasani,  
Edward R. Siuda, ..., Aaron J. Norris,  
Christopher P. Ford, Michael R.  
Bruchas

## Correspondence

bruchasm@wustl.edu

## In Brief

McCall et al. identify locus coeruleus (LC) neuronal activity as a critical mediator of stress-induced anxiety. Selective modulation of LC activity bidirectionally controls anxiety-like and aversive behaviors. Anatomical studies identify amygdalar CRH<sup>+</sup> inputs that modulate LC activity and drive anxiety-like behavior.

# CRH Engagement of the Locus Coeruleus Noradrenergic System Mediates Stress-Induced Anxiety

Jordan G. McCall,<sup>1,2,3,4</sup> Ream Al-Hasani,<sup>1,2,3</sup> Edward R. Siuda,<sup>1,2,3,4</sup> Daniel Y. Hong,<sup>1</sup> Aaron J. Norris,<sup>1</sup> Christopher P. Ford,<sup>5</sup> and Michael R. Bruchas<sup>1,2,3,4,\*</sup>

<sup>1</sup>Division of Basic Research, Department of Anesthesiology, Washington University School of Medicine, St. Louis, MO 63110, USA

<sup>2</sup>Washington University Pain Center, Washington University School of Medicine, St. Louis, MO 63110, USA

<sup>3</sup>Department of Anatomy and Neurobiology, Washington University School of Medicine, St. Louis, MO 63110, USA

<sup>4</sup>Division of Biology and Biomedical Sciences, Washington University School of Medicine, St. Louis, MO 63110, USA

<sup>5</sup>Department of Physiology and Biophysics, Department of Neurosciences, Case Western Reserve University School of Medicine, Cleveland, OH 44106, USA

\*Correspondence: bruchasm@wustl.edu

<http://dx.doi.org/10.1016/j.neuron.2015.07.002>

## SUMMARY

The locus coeruleus noradrenergic (LC-NE) system is one of the first systems engaged following a stressful event. While numerous groups have demonstrated that LC-NE neurons are activated by many different stressors, the underlying neural circuitry and the role of this activity in generating stress-induced anxiety has not been elucidated. Using a combination of *in vivo* chemogenetics, optogenetics, and retrograde tracing, we determine that increased tonic activity of the LC-NE system is necessary and sufficient for stress-induced anxiety and aversion. Selective inhibition of LC-NE neurons during stress prevents subsequent anxiety-like behavior. Exogenously increasing tonic, but not phasic, activity of LC-NE neurons is alone sufficient for anxiety-like and aversive behavior. Furthermore, endogenous corticotropin-releasing hormone<sup>+</sup> (CRH<sup>+</sup>) LC inputs from the amygdala increase tonic LC activity, inducing anxiety-like behaviors. These studies position the LC-NE system as a critical mediator of acute stress-induced anxiety and offer a potential intervention for preventing stress-related affective disorders.

## INTRODUCTION

Acute stress-induced anxiety helps maintain the arousal and vigilance required to sustain attention, accomplish necessary tasks, and avoid repeated exposures to dangerous conditions. Recent basic neuroscience has elucidated circuits throughout the limbic system that are either natively anxiogenic or anxiolytic, building a circuit-based pathology that may yield more selective therapeutic approaches (Felix-Ortiz et al., 2013; Jennings et al., 2013; Kheirbek et al., 2013; Kim et al., 2013a; Tye et al., 2011). However, these limbic structures do not exclusively control anxiogenesis, as elegant recent work reveals parallel systems for anxiety in the septohypothalamic circuitry related to persistent,

stress-induced anxiety (Anthony et al., 2014; Heydendael et al., 2014). Additionally, the majority of these studies propose mechanisms mediated by the fast-acting, small molecule neurotransmitters GABA and glutamate. However, clinically, we know that neuromodulators, such as norepinephrine and various neuropeptides, play pivotal roles in long-term outcomes following stress exposure (Raskind et al., 2013). Here we propose a separate neuromodulatory system underlying immediate, acute stress-induced anxiety.

The locus coeruleus-noradrenergic (LC-NE) system is a small, tightly packed pontine brain region that sends numerous projections to the forebrain and spinal cord. The LC is involved in a broad number of physiological functions, including arousal, memory, cognition, pain processing, behavioral flexibility, and stress reactivity (Berridge and Waterhouse, 2003; Carter et al., 2010; Hickey et al., 2014; Snyder et al., 2012; Tervo et al., 2014; Valentino and Van Bockstaele, 2008; Vazey and Aston-Jones, 2014). The LC system is a major component of the centrally mediated fight-or-flight response with numerous environmental stressors, including social and predator stress, activating the LC-NE system (Bingham et al., 2011; Cassens et al., 1981; Curtis et al., 1997, 2012; Francis et al., 1999; Reyes et al., 2008; Valentino and Van Bockstaele, 2008; Valentino et al., 1991). The response of the LC-NE system to stress is particularly important in the context of stress-induced human neuropsychiatric disorders, such as posttraumatic stress disorder (PTSD) (Olson et al., 2011; Raskind et al., 2013).

Histologically and electrophysiologically identified NE neurons within the LC-NE system of both lightly anesthetized and freely moving rodents, felines, and primates exhibit three distinct activation profiles as follows: (1) low tonic, (2) high tonic, and (3) phasic activity. It has been proposed that these neurons fire differently to determine behavioral flexibility to various environmental challenges. Low-tonic LC discharge (1–2 Hz) is consistent with an awake state (Aston-Jones and Bloom, 1981a; Carter et al., 2010, 2012), whereas phasic burst activity results from distinct sensory stimuli, such as flashes of light, auditory tones, and brief touch (Aston-Jones and Bloom, 1981b; Foote et al., 1980). Stressful events and stimuli shift LC activity toward a high-tonic mode of firing (3–8 Hz), and stress-related neuropeptide release, such as corticotropin-releasing hormone (CRH), is

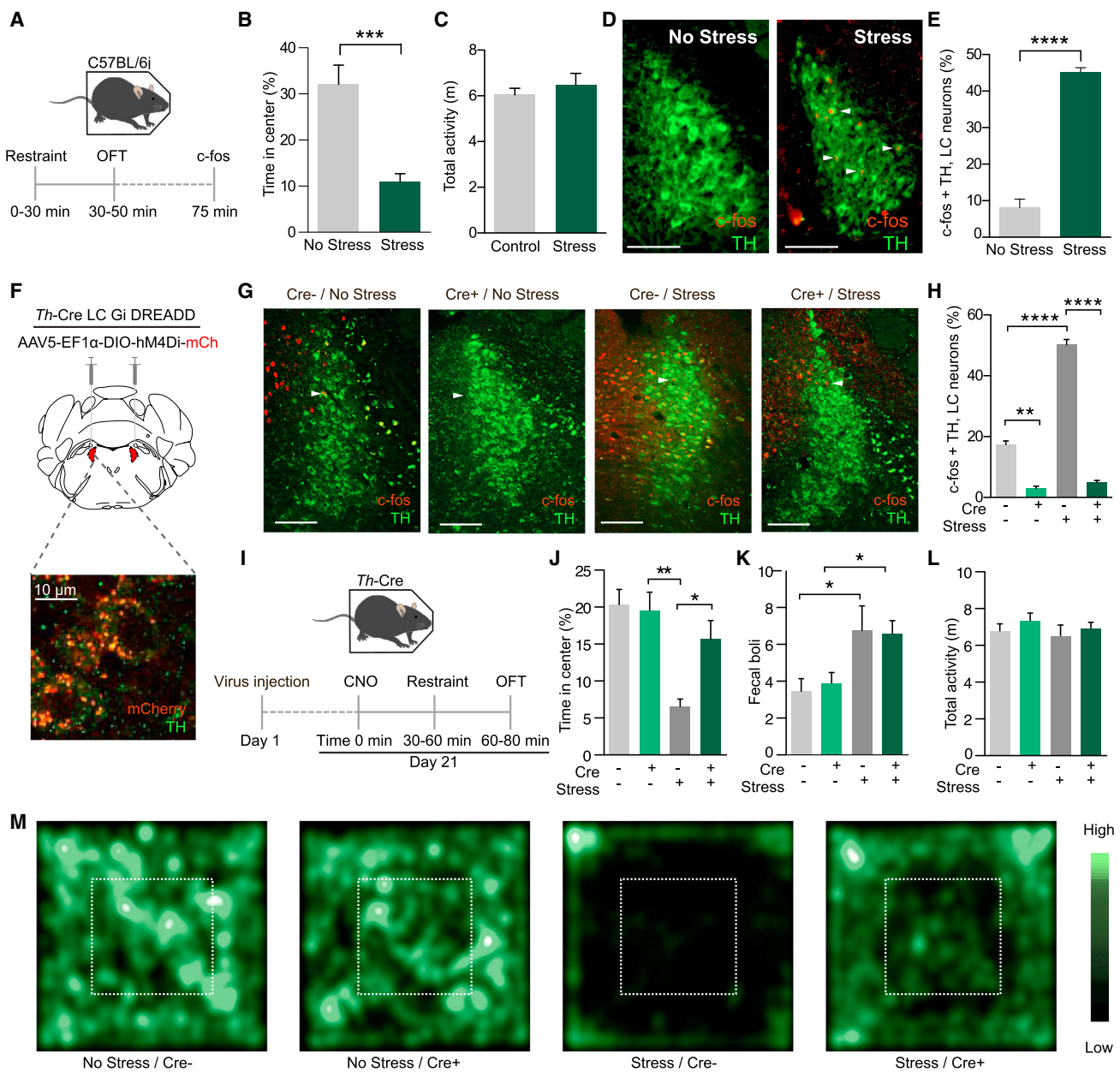


**Figure 1. Chemogenetic Inhibition of LC-NE Neurons Prevents Stress-Induced Anxiety**

(A) Cartoon shows restraint stress-induced anxiety paradigm.

(B and C) Stressed animals spend significantly less time exploring the center of the OFT than non-stressed controls (B) with no change in locomotor activity (C) (data are presented as mean  $\pm$  SEM, n = 7–8/group; Student's t test, p < 0.001).

(D and E) Representative immunohistochemistry (IHC) (D) and quantification (E) show restraint stress increases c-fos immunoreactivity (IR) in LC neurons (red, c-fos; green, tyrosine hydroxylase; arrows, example co-localization). Scale bars, 100  $\mu$ m; data are presented as mean  $\pm$  SEM; n = 3 slices from three animals/group; Student's t test, p < 0.0001). See locomotor activity data in Figure S1.

(F) Cartoon shows viral strategy with high-power confocal image of post-CNO-internalized mCherry expression in LC-NE neurons. Scale bar, 10  $\mu$ m.

(G and H) Representative IHC (G) and quantification (H) show hM4Di inhibition of LC neurons decreases c-fos IR in LC neurons (red, c-fos; green, tyrosine hydroxylase). Scale bars, 100  $\mu$ m; data are presented as mean  $\pm$  SEM; n = 3 slices from three animals/group; one-Way ANOVA, Bonferroni post hoc (No stress/Cre- versus No stress/Cre+ \*\*p < 0.01, No stress/Cre- versus Stress/Cre- \*\*\*\*p < 0.0001, No stress/Cre- versus Stress/Cre+ \*\*\*\*p < 0.0001, No stress/Cre- versus Stress/Cre+ \*\*\*p < 0.001, No stress/Cre+ versus Stress/Cre-, not significant). See also Figure S1.

(I) Cartoon shows LC-NE inhibition paradigm.

(J) Inhibition of LC-NE neurons during stress blocks stress-induced anxiety. Data are presented as mean  $\pm$  SEM; n = 8–13/group; one-Way ANOVA, Newman-Keuls post hoc (No stress/Cre- versus No stress/Cre+ not significant, No stress/Cre- versus Stress/Cre- \*\*p < 0.01, No stress/Cre- versus Stress/Cre+ not significant, No stress/Cre+ versus Stress/Cre- \*\*p < 0.01, No stress/Cre+ versus Stress/Cre+ not significant).

(legend continued on next page)

thought to drive the high-tonic state while simultaneously decreasing phasic firing events (Curtis et al., 1997, 2012; Jendema and Grace, 2004; Page and Abercrombie, 1999; Reyes et al., 2008; Snyder et al., 2012; Valentino and Foote, 1988). Anatomical data support this notion using tract-tracing studies and electron microscopy to suggest that CRH-containing amygdalar monosynaptic projections from the central nucleus of the amygdala (CeA) terminate in the LC (Reyes et al., 2008). Given the importance of CRH in stress-induced behavioral responses, such as dysphoria, anxiety, and aversion (Bruchas et al., 2009; Francis et al., 1999; Gafford et al., 2012; Heinrichs et al., 1994; Koob, 1999; Land et al., 2008), these projections are situated to significantly impact LC neuronal activity. However, the functional consequences of these inputs remain unresolved. We examined the role of this high-tonic activity of LC-NE neurons during stress and defined the endogenous substrates that drive this increased LC-NE activity.

Here we dissect the LC circuitry in the context of stress-induced negative affective behavior. In particular, we use chemogenetics and optogenetics to focus on the role of neural activity of LC-NE neurons in generating these behaviors. We find that LC-NE neurons have increased activity during stress and that blocking this elevated activity suppresses acute stress-induced anxiety. Furthermore, optogenetic activation and release of endogenous amygdalar CRH into the LC promotes anxiety-like and aversive behavior. We report that the LC and its afferent circuitry are critical for encoding and producing stress-induced anxiety.

## RESULTS

### Selective Inhibition of LC-NE Neurons during Stress Suppresses Subsequent Anxiety

Numerous groups have reported that tonic activity of LC-NE neurons increases in response to stress (Bingham et al., 2011; Cassens et al., 1981; Curtis et al., 1997, 2012; Francis et al., 1999; Reyes et al., 2008; Valentino and Van Bockstaele, 2008; Valentino et al., 1991). Others have demonstrated that non-selective pharmacological inactivation or lesions to the LC lessen morphine withdrawal symptoms, prevent footshock-evoked c-fos expression throughout the brain, and disrupt both unconditioned and conditioned aversive responses (Mirzaii-Dizgah et al., 2008; Neophytou et al., 2001; Passerin et al., 2000), but it has previously been untenable to selectively inhibit the activity of only these NE neurons and assess their role in stress-induced behaviors. To examine the role of LC-NE neurons in stress-induced anxiety-like behavior, we implemented a restraint stress paradigm, immediately followed by anxiety testing in the open field test (OFT) (Figure 1A). Following 30 min of restraint stress, wild-type (C57BL/6J) mice produce a robust stress-induced anxiety phenotype and have increased immediate early gene (*cfos*) expression, consistent with increased activ-

ity of LC-NE neurons (Figures 1B–1E; Figure S1A). To determine whether this increase in activity is necessary for the resultant anxiety-like behavior, we selectively targeted the inhibitory designer receptor exclusively activated by designer drug (Gα<sub>i</sub>-coupled; hM4Di DREADD) (Armbruster et al., 2007) to LC-NE neurons by injecting a Cre-dependent AAV into the LC of tyrosine hydroxylase-IRES-Cre mice (*Th-Cre*) (Figure 1F). When the receptor is activated by its ligand, Clozapine-n-oxide (CNO) at a dose previously demonstrated to alter LC activity in rodents (10 mg/kg) (Vazey and Aston-Jones, 2014) prior to stress, there is a significant decrease in stress-induced c-fos<sup>+</sup> in LC-NE neurons, indicating the selective hM4Di DREADD approach is effective at reducing LC-NE activity (Figures 1G and 1H; Figure S1B) during stress.

Next, we used this hM4Di DREADD approach to test whether inhibition of LC-NE neurons during restraint stress can prevent subsequent stress-induced anxiety in the OFT (Figure 1I). Stressed control animals not expressing the Cre-dependent hM4Di (*Th-Cre*<sup>LC:hM4Di−</sup>) showed significant stress-induced anxiety-like behavior compared to unstressed animals regardless of hM4Di expression (*Th-Cre*<sup>LC:hM4Di−</sup> and *Th-Cre*<sup>LC:hM4Di+</sup>), seen in both time spent in the center and entries into the center of the OFT (Figure 1J; Figure S1C). Stressed *Th-Cre*<sup>LC:hM4Di+</sup> animals, however, did not exhibit anxiety-like behavioral responses and instead had behavior similar to and not statistically different from both unstressed *Th-Cre*<sup>LC:hM4Di+</sup> and unstressed *Th-Cre*<sup>LC:hM4Di−</sup> mice (Figure 1J; Figure S1C). Interestingly, hM4Di DREADD-mediated inhibition of LC-NE neurons prior to stress did not alter stress-induced fecal output, suggesting that inhibition of LC-NE neurons suppresses acute stress-induced behavioral anxiety, but leaves other physiological responses intact (Figure 1K; Bruchas et al., 2009; Konturek et al., 2011). Importantly, the hM4Di manipulation had no effect on baseline anxiety levels and none of the manipulations affected locomotor activity (Figures 1L and 1M). These findings suggest that intact LC-NE activity is needed during and after the stress experience to produce an acute stress-induced anxiety state.

### Optogenetic Entrainment of High-Tonic LC-NE Activity

LC-NE neurons are reported to respond vigorously to stress with a robust increase in tonic firing rate (Valentino and Van Bockstaele, 2008). While this physiological response has been observed by many groups, the precise behavioral output of this increase has been previously inaccessible. We selectively targeted channelrhodopsin-2 (ChR2(H134)-eYFP) to LC-NE neurons of *Th-Cre* mice (*Th-Cre*<sup>LC:ChR2</sup>) and observed restricted eYFP labeling to the membranes of NE neurons of the LC (Figures 2A–2C). Slice recordings show that this targeting is sufficient to generate a photocurrent and action potentials in response to 470 nm light (Figures 2D and 2E). To determine whether this strategy could be used to exogenously elevate the tonic firing of LC-NE neurons in a sustained fashion, we

(K) Inhibition of LC-NE neurons has no effect on stress-induced bowel motility. Data are presented as mean ± SEM; n = 8–13/group; one-way ANOVA, Newman-Keuls post hoc (No stress/Cre<sup>−</sup> versus No stress/Cre<sup>+</sup> not significant, No stress/Cre<sup>−</sup> versus Stress/Cre<sup>−</sup>\*p < 0.05, No stress/Cre<sup>−</sup> versus Stress/Cre<sup>+</sup>\*p < 0.05, No stress/Cre<sup>+</sup> versus Stress/Cre<sup>−</sup> not significant, No stress/Cre<sup>+</sup> versus Stress/Cre<sup>+</sup> not significant).

(L) Inhibition of LC-NE neurons has no effect on locomotor activity. Data are presented as mean ± SEM.

(M) Representative heatmaps show activity during OFT.

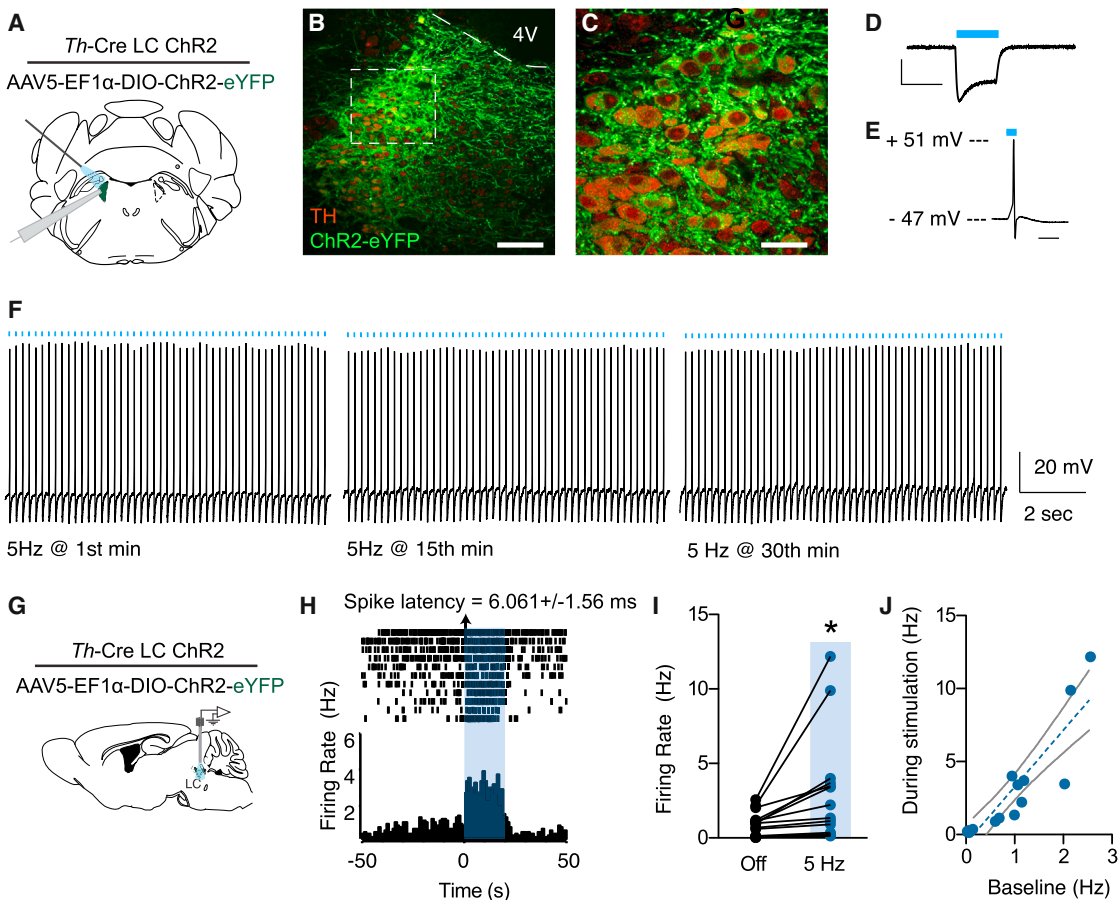


**Figure 2. Optogenetic Targeting to Selectively Drive Tonic LC-NE Activity**

(A) Cartoon shows viral strategy for slice experiments.  
 (B and C) Representative IHC shows selective targeting of ChR2-eYFP to TH<sup>+</sup> LC neurons (red, tyrosine hydroxylase; green, ChR2-eYFP; 4V, fourth ventricle). Scale bars, 100 and 50 μm, respectively.  
 (D and E) Whole-cell current- and voltage-clamp recordings show an LC-NE neuron expressing ChR2. Scale bar, 200 pA × 100 ms (D) and 20 ms (E).  
 (F) Slice recording shows a single LC-NE neuron demonstrating action potentials over 30 min in response to 5 Hz, 470 nm light.  
 (G) Cartoon shows viral and multielectrode delivery for anesthetized, *in vivo* recordings.  
 (H) Peristimulus time histogram (PSTH) shows increased LC neuron firing during a 20-s optical stimulation at 5 Hz.  
 (I) Firing rate of n = 16 cells before and during 5 Hz photostimulation is shown (paired Student's t test, p < 0.01).  
 (J) Correlation of baseline activity to photostimulated activity is shown ( $r = 0.8938$ , p < 0.0001).

performed slice physiology experiments, which demonstrated that LC-NE neurons can fire photostimulated action potentials at 5 Hz for as long as 30 min (Figure 2F). Furthermore, *in vivo* extracellular recordings using a fiber optic-coupled multielectrode array showed that 5 Hz photostimulation produced responses similar to those evoked by stress (Bingham et al., 2011; Curtis et al., 2012; Figures 2G and 2H). Interestingly, putative LC neurons that did not appear to be directly photosensitive (>10-ms spike latency) still increased firing over time, perhaps due to the well-known, tightly coupled nature of neurons in this structure (Alvarez et al., 2002; Figure 2I). Furthermore, indirect responses of these neurons to photostimulation is highly correlated ( $r = 0.89$ , p < 0.0001) to their baseline firing, suggesting that some LC neurons are potentially more intrinsically excited by broader LC activity (Figure 2J). These findings indicate that optogenetic manipulation of LC-NE neurons can be used to sus-

tain tonic firing of LC-NE neurons that mimics their response to stress.

#### Increased LC-NE Tonic Neuronal Firing Is Acutely Anxiogenic

Using the same optogenetic strategy, we examined whether selectively increasing LC-NE tonic firing without a stressor is sufficient to mimic acute stress-induced anxiety-like behaviors. We photostimulated (5 Hz, 10-ms pulse width, 473 nm) LC-NE neurons for the same duration as the restraint stress paradigm and then placed the animals in the OFT (Figures 3A and 3B; Anthony et al., 2014). In this paradigm, *Th-Cre*<sup>LC:ChR2</sup> mice spent significantly less time exploring the center area than Cre<sup>-</sup> controls (Figure 3C), indicating that exogenously increasing LC-NE firing rate can create a persistent anxiety state and reduced locomotor behavior once the stimulation is removed (Figure 3D; Figure S2A).

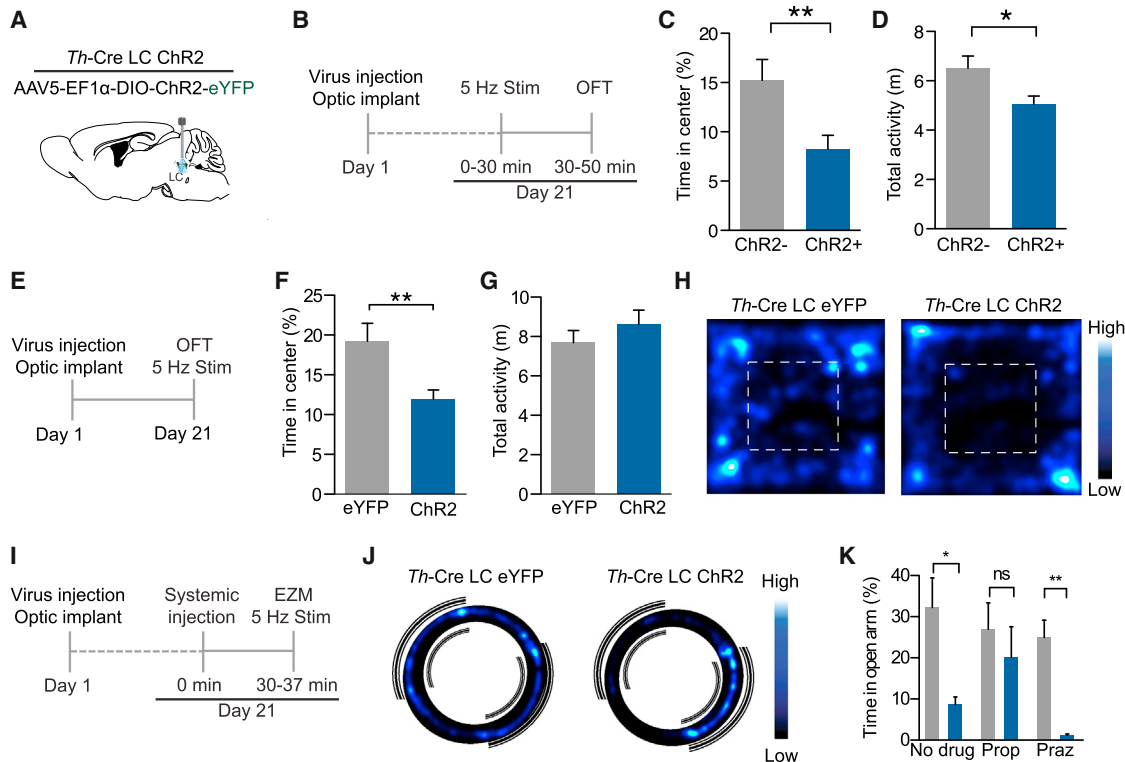


**Figure 3. High-Tonic LC-NE Neuronal Activity Is Sufficient to Induce Anxiety-like Behavior**

(A) Cartoon shows viral and fiber optic delivery.

(B) Calendar shows pre-stimulation OFT studies.

(C) and (D) 5 Hz photostimulation prior to OFT causes an anxiety-like phenotype of ChR2-expressing *Th-Cre*<sup>LC:ChR2+</sup> animals compared to *Th-Cre*<sup>LC:ChR2-</sup> controls (C) (data are presented as mean ± SEM; n = 14–15/group; Mann-Whitney t test, p < 0.01) with a significant decrease in locomotor activity (D) (data are presented as mean ± SEM; n = 14–15/group; Student's t test, p < 0.05).

(E) Calendar shows concurrent stimulation OFT studies.

(F) and (G) 5 Hz photostimulation drives anxiety-like behavior in OFT of *Th-Cre*<sup>LC:ChR2</sup> animals compared to *Th-Cre*<sup>LC:eYFP</sup> controls (F) (data are presented as mean ± SEM; n = 10/group; Student's t test, p < 0.01) with no change in locomotor activity (G) (data are presented as mean ± SEM; n = 10/group).

(H) Representative heatmaps show activity in the OFT. See also Figure S2.

(I) Calendar shows systemic antagonism in EZM studies.

(J) Representative heatmaps show activity in the EZM.

(K) 5 Hz photostimulation drives anxiety-like behavior in EZM of *Th-Cre*<sup>LC:ChR2+</sup> animals compared to *Th-Cre*<sup>LC:ChR2-</sup> controls, which is blocked by β-adrenergic antagonism (Prop), but not α1 antagonism (Praz). Data are presented as mean ± SEM; n = 6–9/group; Kruskal-Wallis one-way ANOVA, \*p < 0.05, \*\*p < 0.01.

To assess whether the photostimulation itself can acutely drive anxiety-like behavior, we tested new animals with photostimulation during two assays of anxiety-like behavior, OFT and elevated zero maze (EZM) (Figure 3E). In the OFT, photostimulated *Th-Cre*<sup>LC:ChR2</sup> mice spent significantly less time exploring the center area than did fluorophore-expressing controls (*Th-Cre*<sup>LC:eYFP</sup>) (Figures 3F and 3G; Figures S2C and S2D). Importantly, concurrent 5 Hz photostimulation did not affect total locomotor activity (Figure 3G; Figure S2B), suggesting 5 Hz LC-NE tonic activity selectively drives anxiety-like behavior.

To determine what downstream receptor systems might be involved in the anxiety-like behavior induced by high-tonic LC-NE activity, we repeated the concurrent photostimulation experiments using the EZM with selective systemic antagonism of either β-adrenergic receptors or α1-adrenergic receptors. At 30 min prior to behavioral testing, we pre-treated animals with either the non-selective β-adrenergic receptor antagonist pro-

pranolol HCl (10 mg/kg, intraperitoneally [i.p.]), the α1-adrenergic antagonist prazosin HCl (1 mg/kg, i.p.), or a vehicle control (Figure 3I). We next photostimulated (5 Hz, 10-ms pulse width, 473 nm) LC-NE neurons during access to EZM (Figures 3J and 3K). As we saw in Figures 3F and 3G, 5 Hz photostimulation in the EZM induced anxiety-like behavior in *Th-Cre*<sup>LC:ChR2+</sup> compared to *Th-Cre*<sup>LC:ChR2-</sup> control animals that do not express ChR2 (Figures 3J and 3K). *Th-Cre*<sup>LC:ChR2+</sup> animals that were pre-treated with propranolol were not significantly different from controls, indicating that systemic β-adrenergic antagonism reversed the effect of LC-NE photostimulation (Figure 3K). Importantly, this was not the case in the animals treated with prazosin (Figure 3K). The blockade of α1-adrenergic receptors in *Th-Cre*<sup>LC:ChR2+</sup> animals still showed an anxiogenic-like behavioral state following photostimulation (Figure S2E). These experiments demonstrate that increasing the tonic firing rate of LC-NE neurons in the absence of a physical stressor is sufficient

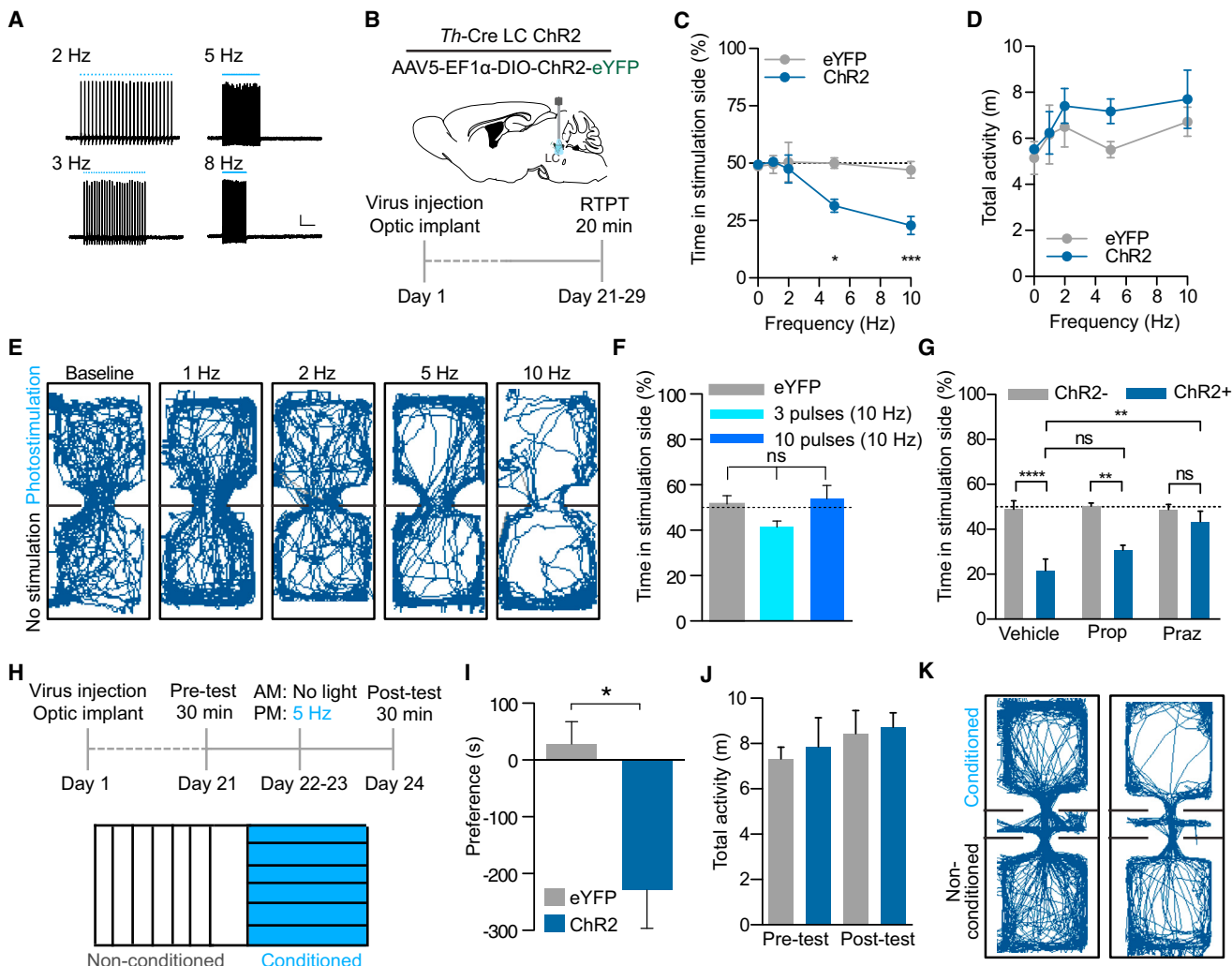


**Figure 4. LC-NE Photostimulation Drives Both Real-Time and Learned Aversions**

- (A) Current-clamp whole-cell recordings at 2, 3, 5, and 8 Hz are shown.
- (B) Cartoon shows viral and fiber optic delivery and calendar of behavioral studies.
- (C and D) Frequency response of RTPT (C) and locomotor activity (D) at 0, 1, 2, 5, and 10 Hz. Data are presented as mean  $\pm$  SEM; n = 6–7/group; two-Way ANOVA, Bonferroni post hoc (5 Hz ChR2 versus 5 Hz eYFP \*p < 0.05, 10 Hz ChR2 versus 10 Hz eYFP \*\*\*p < 0.001).
- (E) Representative traces show behavior at different frequencies.
- (F) Phasic stimulation does not drive aversion (n = 6/group).
- (G) 5 Hz photostimulation causes a real-time place aversion in RTPT of *Th-Cre<sup>LC:ChR2+</sup>* animals compared to *Th-Cre<sup>LC:ChR2-</sup>* controls. This effect is not reversed by propranolol (Prop) pre-treatment, but is by prazosin (Praz). Data are presented as mean  $\pm$  SEM; n = 6–10/group; one-way ANOVA, Bonferroni post hoc, \*\*\*p < 0.0001, \*\*p < 0.01; ns, no significance.
- (H) Timeline and cartoon show 5 Hz CPA experiment.
- (I) Mean preference(s)  $\pm$  SEM is shown, post-test minus pre-test (n = 7–9; Student's t test, p < 0.05).
- (J) No locomotor effect was found in either the pre-test or post-test.
- (K) Representative traces show behavior in the pre-test and post-test. See also Figure S3.

to produce robust anxiety-like behavior, requires NE activity, and is likely mediated by  $\beta$ -adrenergic receptor activity.

### LC-NE Tonic Activity Drives a Frequency-Dependent Real-Time Aversion

Following the observation that increased tonic activity of LC-NE neurons alone is capable of driving anxiety-like behaviors, we next sought to determine whether this activity produced aver-

sion. Following slice electrophysiology experiments that demonstrated dynamic control of LC-NE firing at increasing frequencies while maintaining spike fidelity (Figure 4A), we next sought to determine acute behavioral valence in *Th-Cre<sup>LC:ChR2+</sup>* and *Th-Cre<sup>LC:eYFP</sup>* mice at a range of photostimulation frequencies. To assess the positive or negative valence of the photostimulation, we employed a real-time place-testing (RTPT) assay that triggers photostimulation upon the animal's entry into a chamber void of

salient contextual stimuli (Figure 4B). This assay assesses native behavioral preference to photostimulation; regimes with a negative valence will cause an aversion from and those with a positive valence will drive a preference for the chamber paired with photostimulation (Kim et al., 2013a; Siuda et al., 2015; Stamatakis and Stuber, 2012; Tan et al., 2012). Without photostimulation and at low tonic firing rates similar to alert, awake LC activity (1 and 2 Hz) (Aston-Jones and Bloom, 1981a; Carter et al., 2010, 2012), there was no observable shift in chamber preference compared to baseline or *Th-Cre*<sup>LC:eYFP</sup> control animals (Figure 4C). However, when we increased the frequency of photostimulation to induce a higher tonic firing rate of LC-NE neurons (5 and 10 Hz), we observed a significant frequency-dependent shift away from the photostimulation-paired chamber (Figure 4C). These data suggest that acutely increasing tonic firing of LC-NE neurons elicits a negative valence that is capable of biasing behavior to avoid the increased neuronal activity. As we found in the anxiety-like behavioral assays, there was no change in locomotor activity during any of the frequencies tested (Figures 4D and 4E; Figures S3A and S3B). To determine whether this negative valence was specifically due to increased tonic activity, we implemented the same RTPT assay using two different phasic photostimulation regimes (3 or 10 [10-ms] pulses at 10 Hz upon entry and every 30 s the mouse remained in the chamber). In the phasic photostimulation paradigm, we did not observe any negative or positive valence associated with either phasic regime (Figure 4F; Figures S3C and S3D). This finding is in line with evidence that suggests phasic responses of LC-NE neurons are elicited by salient stimuli rather than stressful events (Aston-Jones and Bloom, 1981b; Sara and Bouret, 2012).

We next determined whether the same systemic antagonism of  $\beta$ -adrenergic receptors that prevented anxiety-like behavior also could prevent the acute negative behavioral valence seen in RTPT. We therefore repeated the experiment at 5 Hz with systemic treatments. Vehicle-treated *Th-Cre*<sup>LC:ChR2+</sup> animals displayed an aversion to the photostimulation-paired chamber compared to *Th-Cre*<sup>LC:ChR2-</sup> controls (Figure 4G). Surprisingly, pre-treatment with propranolol did not block the aversion (Figure 4G). In contrast to our anxiety results, we found that pre-treatment with prazosin blocked the real-time place aversion (Figure 4G). Together, these data suggest that the negative affective behaviors elicited by elevating LC-NE tonic activity are pharmacologically separable.

While the RTPT assay provides clear evidence that increased tonic, but not phasic, activity of LC-NE neurons is acutely aversive, it does not provide information as to whether this activity is encoded and can be later retrieved to inform future behavior. A natural response to a stressful experience would be to avoid the context in which the stress occurred. To test whether increased tonic LC-NE activity produces a learned change in behavior, we employed a Pavlovian conditioned place aversion (CPA) assay (Bruchas et al., 2009; Al-Hasani et al., 2013; Land et al., 2008). In this assay, *Th-Cre*<sup>LC:ChR2</sup> and *Th-Cre*<sup>LC:eYFP</sup> animals are exposed to two distinct visual contexts that have no initial bias. During conditioning, animals do not receive optical stimulation in one context and receive high tonic stimulation (5 Hz, 10-ms pulse widths) in the other context (Figure 4H). When allowed to freely explore both chambers following condi-

tioning, *Th-Cre*<sup>LC:ChR2</sup> animals spent significantly less time in the chamber that was paired with high tonic photostimulation (Figure 4I). In contrast, *Th-Cre*<sup>LC:eYFP</sup> controls did not show a change in behavior from their initial exploration and neither group showed altered locomotor activity (Figures 4J and 4K; Figure S3E). These results suggest that the negative valence and anxiety-like behaviors previously observed during high tonic photostimulation of LC-NE neurons are capable of being learned and influencing future behavior.

### Photostimulation of Galanin-Containing LC-NE Neurons Is Also Sufficient to Elicit Aversion

In addition to the catalytic enzymes necessary for catecholamine production, a majority of LC-NE neurons also produce the neuropeptide galanin (Holets et al., 1988; Melander et al., 1986). Therefore, to further corroborate the results we observed using *Th-Cre* mice, we used mice expressing Cre recombinase under the promoter for galanin (*Gal-Cre*) (Gong et al., 2003; Wu et al., 2014). To validate loci of galanin expression, we crossed these mice to a Cre-conditional tdTomato reporter line developed by the Allen Institute for Brain Science (Ai9) (Madisen et al., 2010). As predicted, we saw dense, local expression in the LC as well as the hypothalamus and brainstem (Figures 5A and 5B). We also observed some tdTomato<sup>+</sup> cells in regions that do not have mRNA for galanin in the adult mouse (cortex, hippocampus, thalamus, and amygdalar structures) (Lein et al., 2007). In each of these regions, we identified transient mRNA expression throughout development (Figure S4). This Cre driver remains, however, a viable tool for selective targeting of the LC (Figure 5C), as seen when we selectively targeted ChR2(H134)-eYFP to LC-NE neurons of *Gal-Cre* mice (*Gal-Cre*<sup>LC:ChR2</sup>) and there was restricted eYFP labeling to the membranes of NE neurons of the LC (Figure 5D; Figure S5). We found that eYFP expression was selective for LC-NE neurons (100% of eYFP-expressing LC neurons were positive for the NE marker dopamine beta hydroxylase [DBH<sup>+</sup>]). However, we found that only 61.48% of LC-NE neurons expressed ChR2(H134)-eYFP in the *Gal-Cre* line—significantly fewer than those in the *Th-Cre* line (Figure 5E; Figure S5).

To test whether tonic photostimulation of this subpopulation of galanin-containing, LC-NE neurons also produces aversion, *Gal-Cre*<sup>LC:ChR2</sup> animals were tested in RTPT with and without photostimulation at 5 Hz. We found that increased tonic LC-NE stimulation in *Gal-Cre*<sup>LC:ChR2</sup> animals produced significant avoidance behavior, consistent with the behavior we observed under the same conditions in the *Th-Cre*<sup>LC:ChR2</sup> mice (Figures 5F and 5G). These experiments corroborate our findings that high tonic stimulation of LC-NE neurons drives an aversive behavioral response, and they suggest that increased activity of the entire population of LC neurons may not be necessary to elicit aversive behavior.

### CRH<sup>+</sup> Neurons from the Central Amygdala Send Dense Projections to the LC

Following observations that exogenously increasing tonic firing of LC-NE neurons is sufficient to drive anxiety-like and aversion behaviors in the absence of stress, we sought to determine the endogenous substrate for increased firing. Previously, CRH

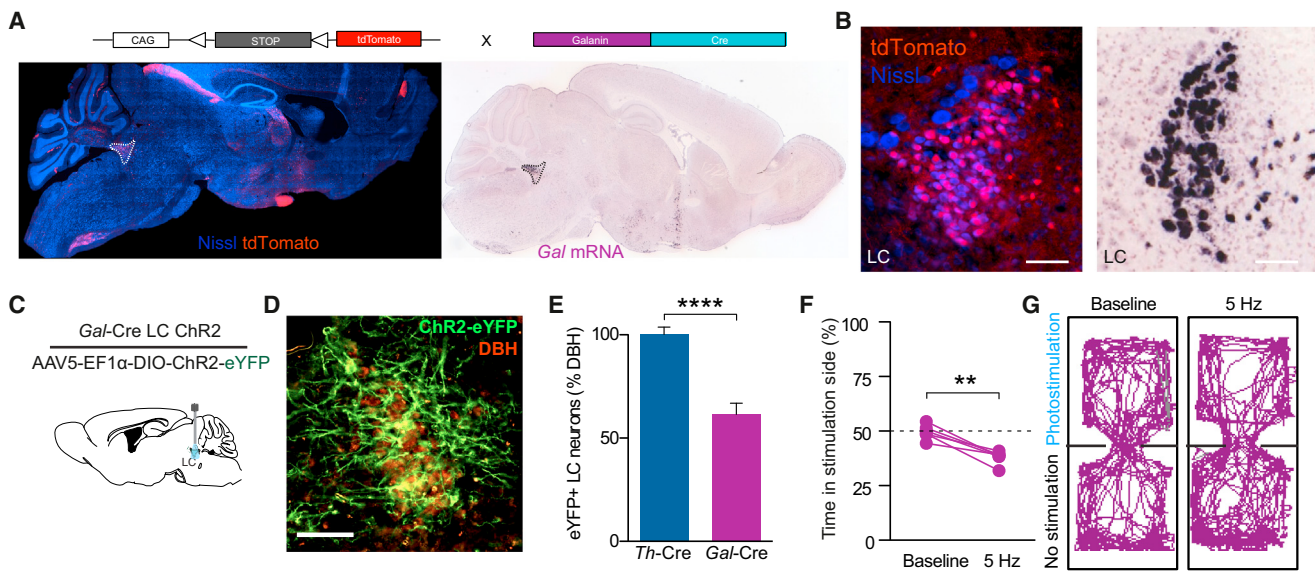


**Figure 5. Galanin-Containing LC-NE Neurons Are Sufficient to Drive Place Aversion**

(A and B) Galanin labeling in *Gal-Cre* × Ai9-*tdTomato* compared to *in situ* images from the Allen Institute for Brain Science in a sagittal section highlighting the presence of galanin in the LC. All images show *tdTomato* (red) and Nissl (blue) staining. See also Figure S4.

(C) Cartoon shows viral and fiber optic delivery.

(D) IHC of ChR2-eYFP targeting to DBH<sup>+</sup> LC neurons is shown. Scale bar, 100 μm.

(E) Quantification of Cre-dependent eYFP viral expression in the LC of *Th-Cre* and *Gal-Cre* mouse lines. Data are presented as mean ± SEM; n = 3 slices from three animals/group; Student's t test, p < 0.0001. See also Figure S5.

(F) 5 Hz stimulation of LC-Gal neurons drives aversion (n = 6; paired Student's t test, p < 0.01).

(G) Representative traces show behavior at different frequencies.

has been suggested as a potential mechanism for stress-induced increases in LC activity (Curtis et al., 1997, 2012; Jedema and Grace, 2004; Page and Abercrombie, 1999; Reyes et al., 2008; Snyder et al., 2012; Valentino and Foote, 1988). Consistent with these studies, we found that systemic antagonism (antalarmin HCl, 10 mg/kg, i.p.) of endogenous CRH action on CRHR1 receptors is sufficient to prevent stress-induced anxiety (Figures 6A–6D; Gafford et al., 2012; Heinrichs et al., 1994; Bruchas et al., 2009).

We next determined whether the action of CRH locally within the LC is responsible for CRH-dependent anxiety-like behavior. To do so, we utilized two retrograde-tracing approaches to examine potential sources of CRH input into the LC. First, we injected the tracer Fluorogold into the LC of C57Bl/6 mice (Figure 6E). This non-selective retrograde-tracing approach revealed known inputs into the LC from the cortex, hypothalamus, and central amygdala—a source of extrahypothalamic CRH (Bouret et al., 2003; Dimitrov et al., 2013; Reyes et al., 2008; Figure 6F; Figure S6). We next used a dual-injection strategy to anatomically isolate LC-projecting, CRH<sup>+</sup> neurons. To do so, we used mice expressing Cre under the promoter for CRH (*Crh-Cre*) mice (Taniguchi et al., 2011). We simultaneously injected a red-labeled retrograde tracer, Cholera Toxin Subunit B (CTB-594) (Conte et al., 2009), to the LC and the green-labeled AAV5-DIO-Ef1α-ChR2(H134)-eYFP to the CeA of these mice (*Crh-Cre*<sup>CeA:ChR2</sup>; Figure 6G). Here we visualized *Crh*<sup>+</sup> neurons in the CeA projection to the LC by observing significant colocalization of both fluorophores in single CeA neurons, indicating that these neurons project to the LC (Figures 6H and 6I).

Finally, to examine CRH<sup>+</sup> terminal innervation of the LC, we only injected the Cre-dependent reporter AAV5-DIO-Ef1α-eYFP in the CeA of *Crh-Cre* mice (Figure 6J). We clearly observed projections from the CeA to the LC in both transverse and coronal sections (Figures 6K–6M; Figures S6F and S6G; Movie S1). These data identify a discrete projection of *Crh*<sup>+</sup> neurons from the CeA to the LC that could act to provide CRH-induced increases in tonic LC activity.

### Photoactivation of CRH<sup>+</sup> Terminals in the LC Causes Increased Tonic Firing of LC Neurons

We next determined the effects of stimulating the CRH terminals locally within the LC. In *Crh-Cre*<sup>CeA-LC:ChR2</sup> mice, we recorded LC activity before, during, and after photostimulation (Figure 7A). The CeA has been reported to spontaneously fire from 2 to 20 Hz (Ciocchi et al., 2010; Veinante and Freund-Mercier, 1998), so we used a 10 Hz photostimulation paradigm to maintain a physiologically relevant frequency. In recordings of 35 putative LC neurons from five different animals, we found a heterogeneous population of responses, including increased firing in a significant proportion of cells (42.8% of observed putative LC units) (Figures 7B–7F; Figure S7A). While the overall sample of neurons significantly increased firing (Figures 7E and 7F), we did observe an equal subset (42.8%) that decreased firing rate during photostimulation (Figure 7H). In cases where the firing rate increased, the mean latency to fire was 344.6 ms, suggesting a neuromodulatory influence (Figures 7F and 7G). Likewise, in cases where the firing rate decreased, the mean latency to

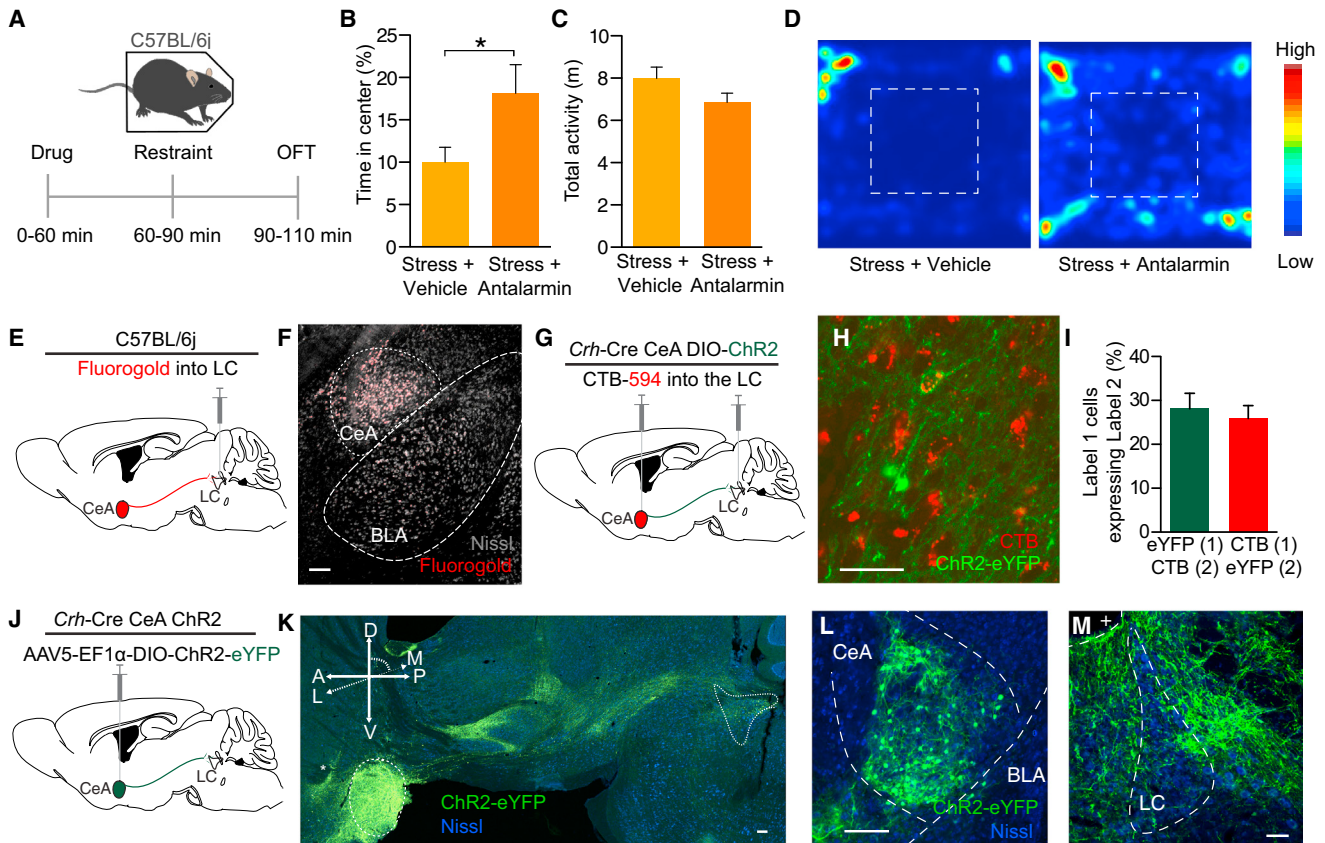


**Figure 6. Identifying a CRH<sup>+</sup> CeA Input to the LC**

(A) Calendar shows the pharmacological experiment.

(B and C) CRF-R1 antagonism blocks stress-induced anxiety-like behavior (B) with no significant effect on locomotor activity (C) ( $n = 6\text{--}8/\text{group}$ ; Student's t test,  $*p < 0.05$ ).

(D) Representative heatmaps show behavior in the OFT.

(E) Cartoon depicts Fluorogold tracing.

(F) Representative image shows robust retrograde labeling of the CeA (Fluorogold, pseudocolored red; Nissl, gray). See also Figure S6.

(G) Cartoon depicts dual-injection tracing for CTB-594 and DIO-ChR2-eYFP.

(H) Representative IHC shows retrograde labeling in CeA of CTB-594 (red) and anterograde labeling of CRH<sup>+</sup> cells (green). Arrow indicates example co-localization.

(I) As shown, ~25% of each label co-labels with the other.

(J) Cartoon depicts anterograde tracing.

(K) 71° off of sagittal slice of *Crh*-Cre mouse expressing DIO-eYFP in the CeA. Image shows intact projections from CeA to LC. Arrow indicates fiber optic placement.

(L and M) Coronal image depict robust eYFP labeling in the CeA and LC of the same mouse. All scale bars, 100  $\mu\text{m}$ ; +fourth ventricle.

fire was 360.0 ms (Figures 7H and 7I). Similar to direct LC-NE photostimulation (Figure 2J), we also observed that the increasing firing rates to *Crh*-Cre<sup>CeA-LC:ChR2</sup> photostimulation are correlated ( $r = 0.70$ ,  $p < 0.0001$ ) to the baseline state of each neuron, indicating that some LC neurons are more excitable by this projection than others (Figure 7J). This observed increase in firing following either stress or exogenous application of CRH is consistent with other reports (Curtis et al., 1997; Je-dema and Grace, 2004; Page and Abercrombie, 1999). However, the slow onset of firing following photostimulation suggested that we did not observe any synaptically mediated events.

To further test for direct, monosynaptic events, we made slice recordings of 35 LC neurons from four mice. While each slice exhibited dense ChR2<sup>+</sup> axonal innervation of the LC (data not

shown but similar to Figure 6M), we never observed any GABA-A inhibitory postsynaptic currents (IPSCs) or AMPA excitatory postsynaptic currents (EPSCs) at a variety of pulse paradigms (10, 20, 50, and 100 Hz) (Figures 7K–7M). While we cannot definitively conclude that there are no direct, fast monosynaptic connections in this projection, these data suggest that the CeA projection mediates action in the LC through either slower neuro-modulatory action or a more complex polysynaptic microcircuit.

### Stimulation of CRH<sup>+</sup> CeA Terminals in the LC Is Aversive and Anxiogenic

We next assessed whether stimulation of these CRH<sup>+</sup> CeA terminals would drive similar behavioral profiles to direct LC-NE stimulation or stress alone. In these experiments, we used

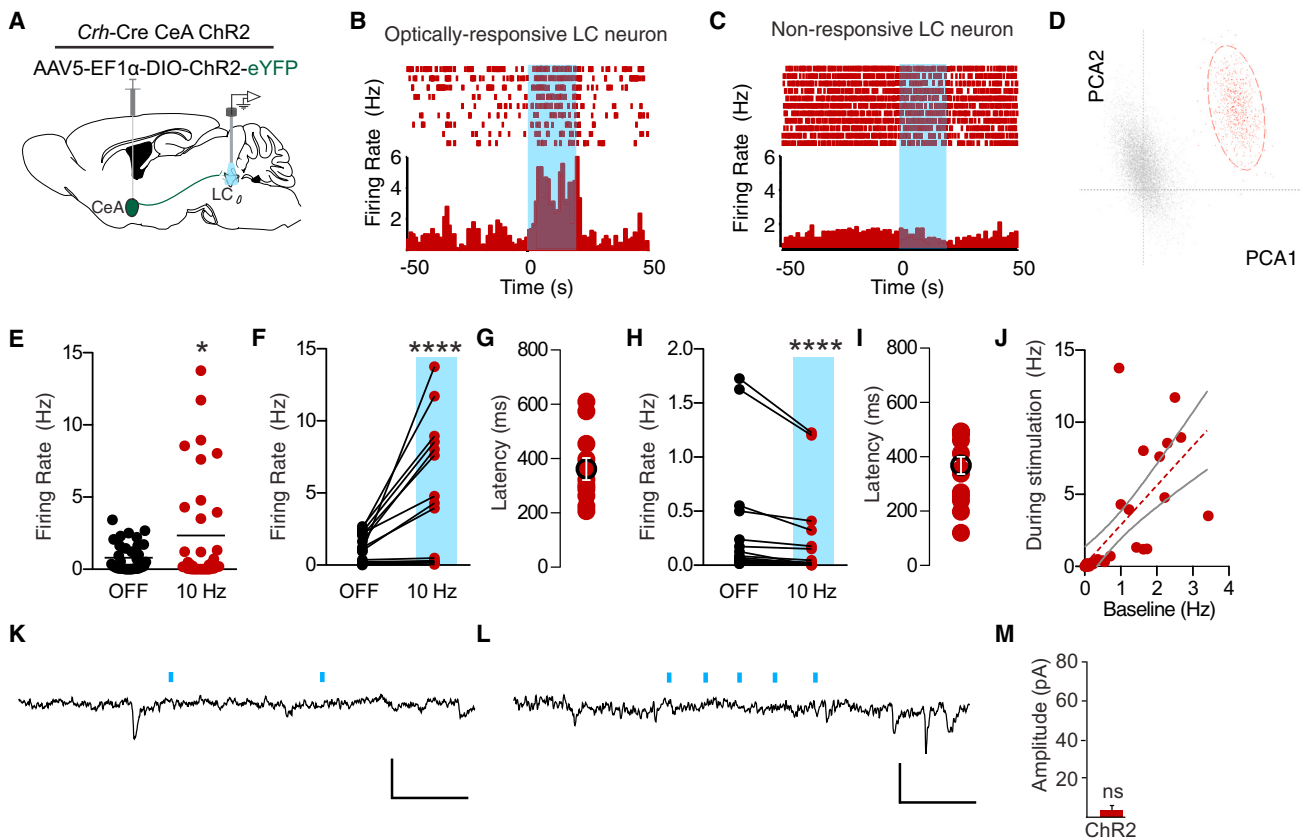


**Figure 7. CRH<sup>+</sup> CeA-LC Terminals Modulate LC Activity and Drive Anxiety through CRFR1 Activation**

(A) Cartoon shows viral and multi-electrode array delivery for anesthetized, *in vivo* recordings.

(B and C) Representative PSTHs show putative LC neurons responding to 20 s of 10 Hz, 10-ms pulse width photostimulation (473 nm, ~10 mW).

(D) Representative principal component analysis plot shows the first two principal components with clear clustering of units.

(E) Total recorded sample shows significant increase in firing rate to 10 Hz photostimulation ( $n = 35$ ; Wilcoxon matched-pairs signed-rank test,  $p < 0.05$ ).

(F) Units ( $n = 15$ ) increase firing rate by >10% during 10 Hz photostimulation (Wilcoxon matched-pairs signed-rank test,  $p < 0.0001$ ).

(G) Response latency following onset of photostimulation for cells that increase firing is shown.

(H) Units ( $n = 15$ ) decrease firing rate by >10% during 10 Hz photostimulation (Wilcoxon matched-pairs signed rank test,  $p < 0.0001$ ). See also Figure S7A.

(I) Response latency following onset of photostimulation for cells that decrease firing is shown.

(J–L) Correlation of baseline activity to activity during photostimulation (J) ( $r = 0.7029$ ,  $p < 0.0001$ ). Representative voltage-clamp traces following 10 Hz, 3-ms photostimulation (K) and 50 Hz, 3-ms photostimulation (L) of *Crh-Cre*<sup>CeA-LC:ChR2</sup> terminals are shown. Scale bars, 30 pA and 50 ms.

(M) Magnitude of the event after the first photostimulation is shown. Data are presented as mean ± SEM;  $n = 35$  cells from four brains.

*Crh-Cre*<sup>CeA-LC:ChR2</sup> and *Crh-Cre*<sup>CeA-LC:eYFP</sup> animals with fiber optic implants over the LC (Figure 8A). Using the same stimulation procedure we used during *in vivo* recordings (10 Hz, 10-ms pulse width), we first observed that photostimulation of CeA-LC CRH<sup>+</sup> terminals conditions a place aversion in *Crh-Cre*<sup>CeA-LC:ChR2</sup> compared to *Crh-Cre*<sup>CeA-LC:eYFP</sup> controls (Figures 8B–8D). We next determined whether this stimulation was sufficient to induce anxiety-like behaviors in the EZM (Figure 8E). In *Crh-Cre*<sup>CeA-LC:ChR2</sup> animals, acute photostimulation produced significant anxiety-like behavior compared to *Crh-Cre*<sup>CeA-LC:eYFP</sup> controls (Figure 8F; Figures S7B and S7C). Importantly, when we locally antagonized CRHRs directly in the LC prior to photostimulation ( $\alpha$ -helical CRF 1  $\mu$ g, intra-LC) this effect was completely reversed, unmasking an anxiolytic phenotype compared to fluorophore-only-expressing antagonist controls, suggesting that CRH release from CeA-LC terminals is the substrate

responsible for the photostimulation-induced anxiety-like behavior (Figure 8F; Figures S7B and S7C). Furthermore, systemic antagonism of CRHR1 (antalarmin HCl, 10 mg/kg, i.p.) prior to photostimulation of *Crh-Cre*<sup>CeA-LC:ChR2</sup> animals prevented the induced anxiety-like behavior (Figure 8G). These results suggest that the CRH<sup>+</sup> projection from the CeA to the LC carries both an aversive and anxiogenic component mediated through CRH<sup>+</sup> activation of CRHR1 in the LC.

## DISCUSSION

The LC-NE system has long been implicated as a key mediator of the central stress response (Koob, 1999). Observational electrophysiological studies across many species identified that LC-NE neurons respond vigorously to stress, and behavioral pharmacology has revealed a potential role for endogenous CRH in

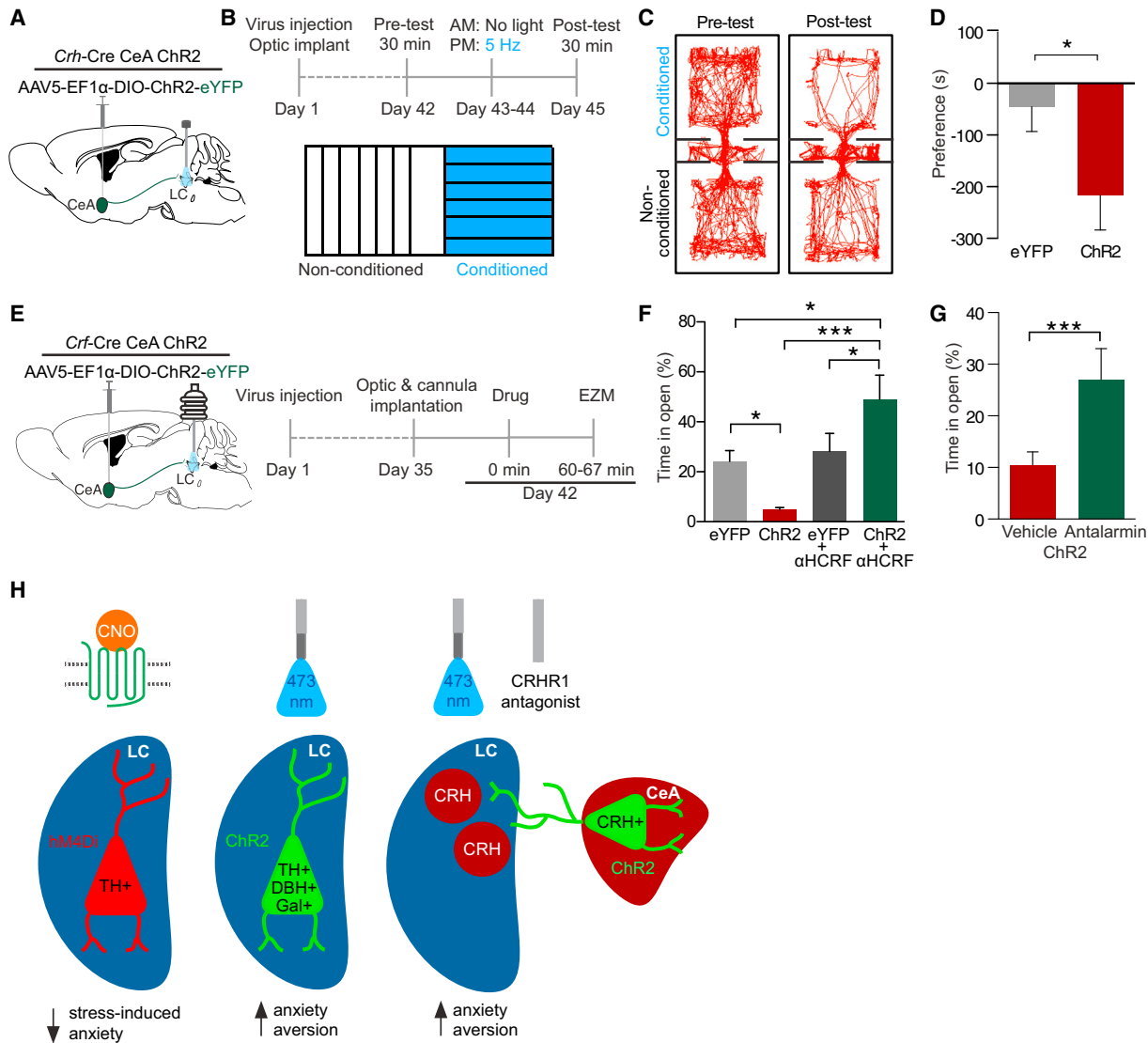


**Figure 8. CRH<sup>+</sup> CeA-LC Terminals Drive Aversion and Anxiety-like Behavior through CRFR1 Activity**

(A) Cartoon shows viral and fiber optic delivery.

(B) Calendar shows CPA behavior.

(C and D) *Crh-Cre*<sup>CeA-LC:ChR2</sup> show a significant CPA compared to *Crh-Cre*<sup>CeA-LC:eYFP</sup> controls. Representative traces show behavior in the pre-test and post-test and mean preference (s)  $\pm$  SEM, post-test minus pre-test ( $n = 10-12$ /group; Student's t test,  $p < 0.05$ ).

(E) Cartoon shows viral, cannula, and fiber optic delivery and calendar of EZM behavior.

(F) 10 Hz photostimulation drives anxiety-like behavior in EZM of *Crh-Cre*<sup>CeA-LC:ChR2</sup> animals compared to *Crh-Cre*<sup>CeA-LC:eYFP</sup> controls, which is reversed by intra-LC  $\alpha$ -helical-CRF ( $\alpha$ HCRF) pretreatment. Data are presented as mean  $\pm$  SEM;  $n = 7$ /group; one-Way ANOVA, Newman-Keuls (*Crh-Cre*<sup>CeA-LC:eYFP</sup> versus *Crh-Cre*<sup>CeA-LC:ChR2</sup> \* $p < 0.05$ , *Cre*<sup>CeA-LC:eYFP</sup> versus *Crh-Cre*<sup>CeA-LC:ChR2+AHCRF</sup> \*\* $p < 0.01$ , *Cre*<sup>CeA-LC:ChR2</sup> versus *Crh-Cre*<sup>CeA-LC:ChR2+AHCRF</sup> \*\*\* $p < 0.001$ ). See also Figures S7B and S7C.

(G) Systemic CRHR1 antagonism reverses photostimulation-induced anxiety-like behavior ( $n = 6-8$ /group; Student's t test,  $p < 0.001$ ).

(H) Model and summary of results are shown. See also Figure S7D.

this response (Bingham et al., 2011; Cassens et al., 1981; Curtis et al., 1997, 2012; Francis et al., 1999; Jedema and Grace, 2004; Page and Abercrombie, 1999; Reyes et al., 2008; Snyder et al., 2012; Valentino et al., 1991; Valentino and Foote, 1988; Valentino and Van Bockstaele, 2008). Here we report that activity of LC-NE neurons is required to elicit acute stress-induced anxiety.

Furthermore, selectively increasing the firing of LC-NE neurons is itself anxiogenic in the absence of stress and can inform future behavior through learned association. Finally, optogenetic stimulation of CRH<sup>+</sup> CeA terminals into the LC replicates the acute anxiogenic and aversive behavioral state of direct LC-NE high tonic stimulation (Figure 8H).

### LC Activity during Stress Is Necessary for Acute Stress-Induced Anxiety

NE tone is important for processing stressful stimuli, encoding fearful events, and deciphering threatening versus non-threatening signals (Aston-Jones et al., 1999; Neophytou et al., 2001; Passerin et al., 2000; Snyder et al., 2012). The findings here that LC-NE activity is required to transmit this information and produce stress-induced anxiety-like behavior extends our understanding of the LC in stress and the fight-or-flight response. Interestingly, inhibition of the LC-NE system without stress did not affect baseline anxiety levels, suggesting that less LC activity is not necessarily anxiolytic. Furthermore, inhibiting LC-NE neurons during stress did not prevent other physiological readouts of stress, such as gastrointestinal motility. Future work will need to determine whether other stress-induced behaviors, such as drug reinstatement and analgesia (Bannister et al., 2009; Al-Hasani et al., 2013; Hickey et al., 2014; Shaham et al., 2000), require increased LC-NE activity.

The chemogenetic inhibition approach used here is temporally restricted due to the kinetics of CNO activity and neuromodulatory effects of DREADDs. We used this approach so as to be agnostic to the timing of the stress-induced activity to capture the period of intense restraint-induced stress as well as the assay-evoked stress inherent in tests of anxiety-like behavior. However, it is not possible to precisely determine when it would be crucial to inhibit LC-NE activity to prevent stress-induced anxiety. Future studies using optogenetic inhibition during either stress or anxiety testing will be needed to ascertain the temporal dynamics of this system. Furthermore, the chemogenetic approach appeared to suppress LC-NE activity below baseline, indicating that some baseline LC-NE activity might be necessary for stress-induced anxiety. However, we do not believe this to be the case given that suppressing LC-NE in unstressed animals did not alter baseline anxiety-like behavior. Additionally, it is possible that only a subset of LC-NE neurons are required for stress-induced anxiety, and previous studies have indicated that the dorsal-ventral axis of the LC has diverse actions (Hickey et al., 2014). Further study is needed to elucidate whether the microanatomy and local neural circuits within the LC play an important role in stress-induced anxiety.

### High-Tonic LC-NE Neuronal Activity Can Initiate Anxiety-like and Aversive Behaviors

Recent studies have used optogenetics for binary control of acute anxiety (Felix-Ortiz et al., 2013; Heydendael et al., 2014; Jennings et al., 2013; Kheirbek et al., 2013; Kim et al., 2013a, 2013b; Tye et al., 2011). These limbic circuits and their projections into the mesolimbic dopamine system have demonstrated rapid onset and offset of anxiety likely mediated by small molecule neurotransmission. Here we demonstrate persistent anxiety-like behavior generated by increasing the tonic activity of the neuromodulatory LC-NE system prior to anxiety testing (similar in timescale to restraint stress) as well as acute anxiety during increased LC-NE activity (control of assay-evoked anxiety). While this activity generates anxiety on a short timescale (seconds to minutes), it is unlikely that the immediate (subsecond timescale) result of high-tonic activity is anxiety. Rather, it is plausible that the LC serves to integrate information from

numerous forebrain and sensory inputs, and, over time, the persistent high-tonic state feeds forward onto previously established anxiety circuits, serving to adjust the gain on these downstream systems to ultimately drive anxiety (Koob, 1999). The amygdala and extended amygdala are candidate regions where feedforward, gain modulation could exist, as there are reciprocal connections between the LC and divisions of the amygdala (Bouret et al., 2003; Buffalari and Grace, 2007; Figure S7D). Importantly, this model of LC modulation of anxiety circuitry is likely an endogenous mechanism given that the removal of the LC-NE system prevents stress-induced anxiety.

The same optogenetic manipulation that incites anxiety also elicits aversive behaviors. These findings suggest that higher tonic frequencies potentially produce anxiety through negative affect. While it is generally thought that anxiety and aversion are both negative affective states, the two behavioral outputs can be neurobiologically distinct (Kim et al., 2013a; Land et al., 2008). This appears to be the case with the LC system. The anxiety-like and real-time aversive components of these behaviors appear to be mediated by different receptor systems (anxiety-like behavior through  $\beta$ -adrenergic receptors and real-time aversion through  $\alpha$ -adrenergic receptors). A circuit-based mechanism for this segregation remains to be determined.

### CRH<sup>+</sup> CeA-LC Terminals Increase Activity and Drive Anxiety through CRFR1 Activation

Anatomical studies first identified the projection from the CeA to the LC (Van Bockstaele et al., 1996, 1998), and recent work has defined these projections to suggest that CeA-LC projections are potentially glutamatergic and carry the neuropeptides dynorphin and CRH (Reyes et al., 2008). Importantly, CRH<sup>+</sup> CeA neurons have been shown to be a part of the protein kinase C  $\delta^-$  subpopulation of CeA neurons recently shown to be distinct from CeA neurons involved in conditioned fear and food consumption (Cai et al., 2014; Haubensak et al., 2010). This CRH<sup>+</sup> projection into the LC has been of particular interest as a source of extrahypothalamic CRH that increases tonic LC firing during stress. The overall population of recorded LC neurons increases tonic firing during photostimulation of CRH<sup>+</sup> CeA-LC terminals, yet we did observe a complex array of responses. The diversity of responses could represent anatomical differentiation of LC neurons. It is possible that non-responding neurons do not receive innervation from the CeA or the local polysynaptic partners, and the difference in responses could be explained by varied expression of cell-surface receptors on postsynaptic neurons. While the literature shows monosynaptic connections exist in this circuit (Reyes et al., 2008), none of our slice physiology or in vivo data suggest any fast-acting neurotransmission. While this could be due to the potential for selection bias inherent in in vivo recordings or an artifact of slower acting neuropeptide/G protein-coupled receptor-mediated transmission, we cannot rule out a polysynaptic mechanism. It is important to note that spatially isolated photostimulation of these terminals in the LC recapitulates the aversion and anxiety-like behaviors observed with both stress and direct LC photostimulation. Furthermore, the anxiety-like behavior can be reversed by either systemic or local antagonism of CRHR1 in the LC, suggesting that photostimulation-induced release of CRH mediates these behaviors.

through action in or very near the LC. While these experiments do not explicitly control for possible optogenetically induced back-propagating action potentials, the anxiogenic to anxiolytic reversal by local CRHR1 blockade suggests the the LC is likely a critical site of action for these behaviors.

Understanding how the vast efferent projection network of the LC facilitates anxiogenesis will be an important next step. We suspect that particular efferent LC-NE projections onto particular postsynaptic receptors likely mediate the observed behavioral outcomes. For example, the LC projects into the lateral septum (LS) and the basolateral amygdala, both of which play key roles in the regulation of stress and anxiety-like behaviors (Anthony et al., 2014; Felix-Ortiz et al., 2013; Tye et al., 2011). While the role of LS neurons in prolonged stress-induced anxiety has been demonstrated clearly (Anthony et al., 2014), future work is needed to investigate whether known LC inputs into the LS (Risold and Swanson, 1997) modulate this system to produce prolonged anxiety. Additionally, the LC has many known projections to other anxiogenic centers, such as the basolateral amygdala and reciprocal projections back to the CeA (Bouret et al., 2003; Buffalari and Grace, 2007), meriting similar investigation (Figure S7D). This circuit-based theory of LC function provides a framework toward understanding other LC functions including attention and arousal.

We report here that stress-induced increases in LC activity are critical for anxiety-like behavior, affirming the LC-NE system as a key mediator of the acute behavioral stress response. Taken together, this study provides a fundamental framework for understanding the mammalian brain circuitry responsible for the innate anxiety response.

## EXPERIMENTAL PROCEDURES

Additional detailed methods are provided in the [Supplemental Experimental Procedures](#).

### Experimental Subjects and Stereotaxic Surgery

Adult (25–35-g) male C57BL/6J, *TH*-IRES-Cre, *Crh*-IRES-Cre, and *Gal*-Cre mice were group-housed, given access to food pellets and water ad libitum, and maintained on a 12:12-hr light/dark cycle (lights on at 7:00 a.m.). All procedures were approved by the Animal Care and Use Committee of Washington University and conformed to NIH guidelines. For surgery, animals were anaesthetized in an induction chamber (4% isoflurane) and placed in a stereotaxic frame where they were maintained at 1%–2% isoflurane. Mice were injected with AAV5-DIO-HM4Di, AAV5-DIO-ChR2 or AAV5-DIO-eYFP, Fluoro-gold, or CTB-594 unilaterally into the LC (coordinates from bregma: –5.45 anterior-posterior [AP], ±1.25 medial-lateral [ML], and –4.00 mm dorsal-ventral [DV]) or the CeA (–1.25 AP, ±2.75 ML, and –4.75 DV). Mice were then implanted with metal cannula or fiber optic implants (adjusted from viral injection 0.00 AP, ±0.25 ML, and +1.00 DV) (Carter et al., 2010).

### Immunohistochemistry

Immunohistochemistry was performed as previously described (Al-Hasani et al., 2013; Kim et al., 2013b).

### Behavior

All behaviors were performed within a sound-attenuated room maintained at 23°C at least 1 week after habituation to the holding room and the final surgery. Lighting was stabilized at ~250 lux for anxiety-like behaviors and at ~1,500 lux for aversion behaviors. Movements were video recorded and analyzed using Ethovision 8.5 (Noldus Information Technologies, RRID: rid\_000100).

### Stress-Induced Anxiety Paradigm

Mice were immobilized in modified disposable conical tubes once for 30 min and were then immediately transferred to the open field. For the hM4Di experiments, mice were injected with CNO (10 mg/kg, i.p., 30 min prior to restraint) (Vazey and Aston-Jones, 2014). For the CRF antagonism experiment, mice were injected with antalarmin HCl (10 mg/kg, i.p., 30 min prior to restraint).

### OFT

The OFT was performed in a 2,500 cm<sup>2</sup> enclosure for 20 min (stress-induced or pre-stimulation experiments); the center was defined as a square of 50% of the total OFT area. For acute optogenetic experiments, *Th*-Cre<sup>LC:ChR2</sup> or *Th*-Cre<sup>LC:eYFP</sup> mice were allowed to roam for 21 min. Photostimulation alternated off and on (5 Hz, 10-ms width, ~10-mW light power) in 3-min bins.

### EZM

The EZM testing was performed as described previously (Bruchas et al., 2009; Kim et al., 2013b). *Th*-Cre animals received 5 Hz (10-ms width) and *Crh*-Cre animals received 10 Hz (10-ms width) photostimulation (~10-mW light power). For the CRFR1 antagonism experiments, mice were infused into the LC with α-helical CRF (1 μg, intra-LC, 1 hr prior to behavior; Tocris) or antalarmin HCl (10 mg/kg, i.p., 30 min prior to behavior; Sigma).

### Conditioned Place Aversion

Mice were trained in an unbiased, balanced three-compartment conditioning apparatus as described previously (Bruchas et al., 2009; Al-Hasani et al., 2013; Land et al., 2008).

### Real-Time Place Testing

Animals were placed in a custom-made unbiased, balanced two-compartment conditioning apparatus (52.5 × 25.5 × 25.5 cm) as described previously (Siuda et al., 2015). During a 20-min trial, entry into one compartment triggered photostimulation of various frequencies (0, 1, 2, 5, 10 Hz, etc.) while the animal remained in the light-paired chamber, and entry into the other chamber ended photostimulation.

### Slice Electrophysiology

Following anesthesia, horizontal midbrain slices containing the LC (240 μm) were cut in ice-cold cutting solution and incubated post-cutting at 35°C in oxygenated ACSF solution with 10 μM MK-801 for 45 min before recording. Following incubation, slices were placed in a recording chamber and perfused with ACSF (34 ± 2°C) containing 100 μM picrotoxin, 10 μM DNQX, and 1 μM idazoxan at 2 ml/min. Whole-cell current-clamp recordings were made as described previously (Courtney and Ford, 2014). Wide-field activation of ChR2 was activated with collimated light from an LED (470 nm, ~1 mW) through the 40× water immersion objective. Patch pipettes (1.5–2 MW) were pulled from borosilicate glass (World Precision Instruments). To examine synaptic events driven by optogenetic stimulation (3-ms pulses) of CRH terminals in the LC, recordings were made in the absence of synaptic receptor antagonists. To confirm that photostimulation of terminals arising from the CeA did not evoke measurable synaptic events, recordings also were made in a subset of trials (n = 5) in the presence of TTX (500 nM), 4-AP (100 μM), and antalarmin (10 μM). All solutions can be found in the [Supplemental Experimental Procedures](#).

### In Vivo Electrophysiology

A 16-channel array (35-μm tungsten wires, 150-μm spacing between wires, 150-μm spacing between rows; Innovative Physiological) was epoxied to a fiber optic and lowered into the LC of lightly (<1% isoflurane) anesthetized *Th*-Cre<sup>LC:ChR2</sup> or *Crh*-Cre<sup>CeA-LC:ChR2</sup> animals. Voltages from each electrode were bandpass-filtered with activity between 250 and 8,000 Hz analyzed as spikes. LC cells were selected based on stereotaxic position, baseline activity, and toe pinch response. The signal was amplified and digitally converted (Omniplex and PlexControl, Plexon), and spikes were sorted using principal component analysis and/or evaluation of t-distribution with expectation maximization (Offline sorter, Plexon). Sorted units were analyzed with NeuroExplorer 3.0 (RRID: nif-0000-10382) and timestamps were exported for further analysis in Microsoft Excel and MATLAB 7.12 (RRID: nlx\_153890).

**Data Analysis/Statistics**

All data are expressed as mean  $\pm$  SEM. In data that were normally distributed, differences between groups were determined using independent t tests or one-way ANOVA, or two-way ANOVAs followed by post hoc comparisons if the main effect was significant at  $p < 0.05$ . In cases where data failed the D'Agostino and Pearson omnibus normality test, non-parametric analyses were used. Statistical analyses were conducted using Prism 5.0 (GraphPad).

**SUPPLEMENTAL INFORMATION**

Supplemental Information includes Supplemental Experimental Procedures, seven figures, and one movie and can be found with this article online at <http://dx.doi.org/10.1016/j.neuron.2015.07.002>.

**AUTHOR CONTRIBUTIONS**

Conceptualization, J.G.M. and M.R.B.; Methodology, J.G.M., R.A., E.R.S., C.P.F., and M.R.B.; Investigation, J.G.M., C.P.F., R.A., E.R.S., D.Y.H., and A.J.N.; Writing – Original Draft, Review & Editing, J.G.M. and M.R.B.; Funding acquisition, M.R.B.; Supervision, C.P.F.; Project administration, M.R.B.

**ACKNOWLEDGMENTS**

This work is supported by the National Institute on Drug Abuse (NIDA) R21 DA035144 (M.R.B.), McDonnell Center for Systems Neuroscience (M.R.B.), NIDA R01 DA035821 (C.P.F.), NIMH F31 MH101956 (J.G.M.), NIDA K99 DA038725 (R.A.), and Washington University School of Medicine Division of Biological and Biomedical Sciences (J.G.M.). We thank the M.R.B laboratory, in particular Blessan Sebastian, William Planer, Audra Foshage, and Lamley Lawson, for helpful insights, discussions, and technical support. We especially thank Robert W. Gereau IV, Erik D. Herzog, Timothy E. Holy, Joseph D. Dougherty, and Vijay K. Samineni for helpful discussions. We thank Karl Deisseroth (Stanford University) for the channelrhodopsin-2 (H134) construct, Garret Stuber (University of North Carolina) for the *Th*-IRES-Cre mice, and Max Kelz (University of Pennsylvania) for the *Gal*-Cre mice. We also thank The Washington University School of Medicine HOPE Center viral vector core (National Institute of Neurological Disorders and Stroke [NINDS], P30NS057105) and Bakewell Neuroimaging Laboratory.

Received: February 5, 2015

Revised: June 9, 2015

Accepted: July 1, 2015

Published: July 23, 2015

**REFERENCES**

- Al-Hasani, R., McCall, J.G., Foshage, A.M., and Bruchas, M.R. (2013). Locus coeruleus kappa-opioid receptors modulate reinstatement of cocaine place preference through a noradrenergic mechanism. *Neuropharmacology* 38, 2484–2497.
- Alvarez, V.A., Chow, C.C., Van Bockstaele, E.J., and Williams, J.T. (2002). Frequency-dependent synchrony in locus ceruleus: role of electrotonic coupling. *Proc. Natl. Acad. Sci. USA* 99, 4032–4036.
- Anthony, T.E., Dee, N., Bernard, A., Lerchner, W., Heintz, N., and Anderson, D.J. (2014). Control of stress-induced persistent anxiety by an extra-amygdala septohypothalamic circuit. *Cell* 156, 522–536.
- Armbuster, B.N., Li, X., Pausch, M.H., Herlitze, S., and Roth, B.L. (2007). Evolving the lock to fit the key to create a family of G protein-coupled receptors potently activated by an inert ligand. *Proc. Natl. Acad. Sci. USA* 104, 5163–5168.
- Aston-Jones, G., and Bloom, F.E. (1981a). Activity of norepinephrine-containing locus coeruleus neurons in behaving rats anticipates fluctuations in the sleep-waking cycle. *J. Neurosci.* 1, 876–886.
- Aston-Jones, G., and Bloom, F.E. (1981b). Norepinephrine-containing locus coeruleus neurons in behaving rats exhibit pronounced responses to non-noxious environmental stimuli. *J. Neurosci.* 1, 887–900.
- Aston-Jones, G., Rajkowski, J., and Cohen, J. (1999). Role of locus coeruleus in attention and behavioral flexibility. *Biol. Psychiatry* 46, 1309–1320.
- Bannister, K., Bee, L.A., and Dickenson, A.H. (2009). Preclinical and early clinical investigations related to monoaminergic pain modulation. *Neurotherapeutics* 6, 703–712.
- Berridge, C.W., and Waterhouse, B.D. (2003). The locus coeruleus-noradrenergic system: modulation of behavioral state and state-dependent cognitive processes. *Brain Res. Brain Res. Rev.* 42, 33–84.
- Bingham, B., McFadden, K., Zhang, X., Bhatnagar, S., Beck, S., and Valentino, R. (2011). Early adolescence as a critical window during which social stress distinctly alters behavior and brain norepinephrine activity. *Neuropharmacology* 56, 896–909.
- Bouret, S., Duvel, A., Onat, S., and Sara, S.J. (2003). Phasic activation of locus ceruleus neurons by the central nucleus of the amygdala. *J. Neurosci.* 23, 3491–3497.
- Bruchas, M.R., Land, B.B., Lemos, J.C., and Chavkin, C. (2009). CRF1-R activation of the dynorphin/kappa opioid system in the mouse basolateral amygdala mediates anxiety-like behavior. *PLoS ONE* 4, e8528.
- Buffalari, D.M., and Grace, A.A. (2007). Noradrenergic modulation of basolateral amygdala neuronal activity: opposing influences of alpha-2 and beta receptor activation. *J. Neurosci.* 27, 12358–12366.
- Cai, H., Haubensak, W., Anthony, T.E., and Anderson, D.J. (2014). Central amygdala PKC- $\delta$ (+) neurons mediate the influence of multiple anorexigenic signals. *Nat. Neurosci.* 17, 1240–1248.
- Carter, M.E., Yizhar, O., Chikahisa, S., Nguyen, H., Adamantidis, A., Nishino, S., Deisseroth, K., and de Lecea, L. (2010). Tuning arousal with optogenetic modulation of locus coeruleus neurons. *Nat. Neurosci.* 13, 1526–1533.
- Carter, M.E., Brill, J., Bonnavion, P., Huguenard, J.R., Huerta, R., and de Lecea, L. (2012). Mechanism for Hypocretin-mediated sleep-to-wake transitions. *Proc. Natl. Acad. Sci. USA* 109, E2635–E2644.
- Cassens, G., Kuruc, A., Roffman, M., Orsulak, P.J., and Schildkraut, J.J. (1981). Alterations in brain norepinephrine metabolism and behavior induced by environmental stimuli previously paired with inescapable shock. *Behav. Brain Res.* 2, 387–407.
- Ciocchi, S., Herry, C., Grenier, F., Wolff, S.B.E., Letzkus, J.J., Vlachos, I., Ehrlich, I., Sprengel, R., Deisseroth, K., Stadler, M.B., et al. (2010). Encoding of conditioned fear in central amygdala inhibitory circuits. *Nature* 468, 277–282.
- Conte, W.L., Kamishina, H., and Reep, R.L. (2009). Multiple neuroanatomical tract-tracing using fluorescent Alexa Fluor conjugates of cholera toxin subunit B in rats. *Nat. Protoc.* 4, 1157–1166.
- Courtney, N.A., and Ford, C.P. (2014). The timing of dopamine- and noradrenalin-mediated transmission reflects underlying differences in the extent of spillover and pooling. *J. Neurosci.* 34, 7645–7656.
- Curtis, A.L., Lechner, S.M., Pavcovich, L.A., and Valentino, R.J. (1997). Activation of the locus coeruleus noradrenergic system by intracerebral microinfusion of corticotropin-releasing factor: effects on discharge rate, cortical norepinephrine levels and cortical electroencephalographic activity. *J. Pharmacol. Exp. Ther.* 281, 163–172.
- Curtis, A.L., Leiser, S.C., Snyder, K., and Valentino, R.J. (2012). Predator stress engages corticotropin-releasing factor and opioid systems to alter the operating mode of locus coeruleus norepinephrine neurons. *Neuropharmacology* 62, 1737–1745.
- Dimitrov, E.L., Yanagawa, Y., and Usdin, T.B. (2013). Forebrain GABAergic projections to locus coeruleus in mouse. *J. Comp. Neurol.* 521, 2373–2397.
- Felix-Ortiz, A.C., Beyeler, A., Seo, C., Leppla, C.A., Wildes, C.P., and Tye, K.M. (2013). BLA to vHPC inputs modulate anxiety-related behaviors. *Neuron* 79, 658–664.

- Foote, S.L., Aston-Jones, G., and Bloom, F.E. (1980). Impulse activity of locus coeruleus neurons in awake rats and monkeys is a function of sensory stimulation and arousal. *Proc. Natl. Acad. Sci. USA* 77, 3033–3037.
- Francis, D.D., Caldji, C., Champagne, F., Plotsky, P.M., and Meaney, M.J. (1999). The role of corticotropin-releasing factor–norepinephrine systems in mediating the effects of early experience on the development of behavioral and endocrine responses to stress. *Biol. Psychiatry* 46, 1153–1166.
- Gafford, G.M., Guo, J.-D., Flandreau, E.I., Hazra, R., Rainnie, D.G., and Ressler, K.J. (2012). Cell-type specific deletion of GABA(A) $\alpha$ 1 in corticotropin-releasing factor-containing neurons enhances anxiety and disrupts fear extinction. *Proc. Natl. Acad. Sci. USA* 109, 16330–16335.
- Gong, S., Zheng, C., Doughty, M.L., Losos, K., Didkovsky, N., Schambra, U.B., Nowak, N.J., Joyner, A., Leblanc, G., Hatten, M.E., and Heintz, N. (2003). A gene expression atlas of the central nervous system based on bacterial artificial chromosomes. *Nature* 425, 917–925.
- Haubensak, W., Kunwar, P.S., Cai, H., Ciocchi, S., Wall, N.R., Ponnusamy, R., Biag, J., Dong, H.-W., Deisseroth, K., Callaway, E.M., et al. (2010). Genetic dissection of an amygdala microcircuit that gates conditioned fear. *Nature* 468, 270–276.
- Heinrichs, S.C., Menzaghi, F., Pich, E.M., Baldwin, H.A., Rassnick, S., Britton, K.T., and Koob, G.F. (1994). Anti-stress action of a corticotropin-releasing factor antagonist on behavioral reactivity to stressors of varying type and intensity. *Neuropsychopharmacology* 11, 179–186.
- Heydendael, W., Sengupta, A., Beck, S., and Bhatnagar, S. (2014). Optogenetic examination identifies a context-specific role for orexins/hypocretins in anxiety-related behavior. *Physiol. Behav.* 130, 182–190.
- Hickey, L., Li, Y., Fyson, S.J., Watson, T.C., Perrins, R., Hewinson, J., Teschemacher, A.G., Furue, H., Lum, B.M., and Pickering, A.E. (2014). Optoactivation of locus ceruleus neurons evokes bidirectional changes in thermal nociception in rats. *J. Neurosci.* 34, 4148–4160.
- Holets, V.R., Hökfelt, T., Rökaeus, A., Terenius, L., and Goldstein, M. (1988). Locus coeruleus neurons in the rat containing neuropeptide Y, tyrosine hydroxylase or galanin and their efferent projections to the spinal cord, cerebral cortex and hypothalamus. *Neuroscience* 24, 893–906.
- Jedema, H.P., and Grace, A.A. (2004). Corticotropin-releasing hormone directly activates noradrenergic neurons of the locus ceruleus recorded in vitro. *J. Neurosci.* 24, 9703–9713.
- Jennings, J.H., Sparta, D.R., Stamatakis, A.M., Ung, R.L., Pleil, K.E., Kash, T.L., and Stuber, G.D. (2013). Distinct extended amygdala circuits for divergent motivational states. *Nature* 496, 224–228.
- Kheirbek, M.A., Drew, L.J., Burghardt, N.S., Costantini, D.O., Tannenholz, L., Ahmari, S.E., Zeng, H., Fenton, A.A., and Hen, R. (2013). Differential control of learning and anxiety along the dorsoventral axis of the dentate gyrus. *Neuron* 77, 955–968.
- Kim, S.-Y., Adhikari, A., Lee, S.Y., Marshel, J.H., Kim, C.K., Mallory, C.S., Lo, M., Pak, S., Mattis, J., Lim, B.K., et al. (2013a). Diverging neural pathways assemble a behavioural state from separable features in anxiety. *Nature* 496, 219–223.
- Kim, T.I., McCall, J.G., Jung, Y.H., Huang, X., Siuda, E.R., Li, Y., Song, J., Song, Y.M., Pao, H.A., Kim, R.-H., et al. (2013b). Injectable, cellular-scale optoelectronics with applications for wireless optogenetics. *Science* 340, 211–216.
- Konturek, P.C., Brzozowski, T., and Konturek, S.J. (2011). Stress and the gut: pathophysiology, clinical consequences, diagnostic approach and treatment options. *J. Physiol. Pharmacol.* 62, 591–599.
- Koob, G.F. (1999). Corticotropin-releasing factor, norepinephrine, and stress. *Biol. Psychiatry* 46, 1167–1180.
- Land, B.B., Bruchas, M.R., Lemos, J.C., Xu, M., Melief, E.J., and Chavkin, C. (2008). The dysphoric component of stress is encoded by activation of the dynorphin kappa-opioid system. *J. Neurosci.* 28, 407–414.
- Lein, E.S., Hawrylycz, M.J., Ao, N., Ayres, M., Bensinger, A., Bernard, A., Boe, A.F., Boguski, M.S., Brockway, K.S., Byrnes, E.J., et al. (2007). Genome-wide atlas of gene expression in the adult mouse brain. *Nature* 445, 168–176.
- Madisen, L., Zwingman, T.A., Sunkin, S.M., Oh, S.W., Zariwala, H.A., Gu, H., Ng, L.L., Palmiter, R.D., Hawrylycz, M.J., Jones, A.R., et al. (2010). A robust and high-throughput Cre reporting and characterization system for the whole mouse brain. *Nat. Neurosci.* 13, 133–140.
- Melander, T., Hökfelt, T., and Rökaeus, A. (1986). Distribution of galaninlike immunoreactivity in the rat central nervous system. *J. Comp. Neurol.* 248, 475–517.
- Mirzaei-Dizgah, I., Karimian, S.M., Hajimashhadi, Z., Riahi, E., and Ghasemi, T. (2008). Attenuation of morphine withdrawal signs by muscimol in the locus coeruleus of rats. *Behav. Pharmacol.* 19, 171–175.
- Neophytou, S.I., Aspley, S., Butler, S., Beckett, S., and Marsden, C.A. (2001). Effects of lesioning noradrenergic neurones in the locus coeruleus on conditioned and unconditioned aversive behaviour in the rat. *Prog. Neuropsychopharmacol. Biol. Psychiatry* 25, 1307–1321.
- Olson, V.G., Rockett, H.R., Reh, R.K., Redila, V.A., Tran, P.M., Venkov, H.A., Defino, M.C., Hague, C., Peskind, E.R., Szot, P., and Raskind, M.A. (2011). The role of norepinephrine in differential response to stress in an animal model of posttraumatic stress disorder. *Biol. Psychiatry* 70, 441–448.
- Page, M.E., and Abercrombie, E.D. (1999). Discrete local application of corticotropin-releasing factor increases locus coeruleus discharge and extracellular norepinephrine in rat hippocampus. *Synapse* 33, 304–313.
- Passerin, A.M., Cano, G., Rabin, B.S., Delano, B.A., Napier, J.L., and Sved, A.F. (2000). Role of locus coeruleus in foot shock-evoked Fos expression in rat brain. *Neuroscience* 101, 1071–1082.
- Raskind, M.A., Peterson, K., Williams, T., Hoff, D.J., Hart, K., Holmes, H., Homas, D., Hill, J., Daniels, C., Calohan, J., et al. (2013). A trial of prazosin for combat trauma PTSD with nightmares in active-duty soldiers returned from Iraq and Afghanistan. *Am. J. Psychiatry* 170, 1003–1010.
- Reyes, B.A., Drolet, G., and Van Bockstaele, E.J. (2008). Dynorphin and stress-related peptides in rat locus coeruleus: contribution of amygdalar efferents. *J. Comp. Neurol.* 508, 663–675.
- Risold, P.Y., and Swanson, L.W. (1997). Chemoarchitecture of the rat lateral septal nucleus. *Brain Res. Brain Res. Rev.* 24, 91–113.
- Sara, S.J., and Bouret, S. (2012). Orienting and reorienting: the locus coeruleus mediates cognition through arousal. *Neuron* 76, 130–141.
- Shaham, Y., Highfield, D., Delfs, J., Leung, S., and Stewart, J. (2000). Clonidine blocks stress-induced reinstatement of heroin seeking in rats: an effect independent of locus coeruleus noradrenergic neurons. *Eur. J. Neurosci.* 12, 292–302.
- Siuda, E.R., Copits, B.A., Schmidt, M.J., Baird, M.A., Al-Hasani, R., Planer, W.J., Funderburk, S.C., McCall, J.G., Gereau, R.W., 4th, and Bruchas, M.R. (2015). Spatiotemporal control of opioid signaling and behavior. *Neuron* 86, 923–935.
- Snyder, K., Wang, W.-W., Han, R., McFadden, K., and Valentino, R.J. (2012). Corticotropin-releasing factor in the norepinephrine nucleus, locus coeruleus, facilitates behavioral flexibility. *Neuropsychopharmacology* 37, 520–530.
- Stamatakis, A.M., and Stuber, G.D. (2012). Activation of lateral habenula inputs to the ventral midbrain promotes behavioral avoidance. *Nat. Neurosci.* 15, 1105–1107.
- Tan, K.R., Yvon, C., Turiault, M., Mirzabekov, J.J., Doehner, J., Labouëbe, G., Deisseroth, K., Tye, K.M., and Lüscher, C. (2012). GABA neurons of the VTA drive conditioned place aversion. *Neuron* 73, 1173–1183.
- Taniguchi, H., He, M., Wu, P., Kim, S., Paik, R., Sugino, K., Kvitsiani, D., Fu, Y., Lu, J., Lin, Y., et al. (2011). A resource of Cre driver lines for genetic targeting of GABAergic neurons in cerebral cortex. *Neuron* 71, 995–1013.
- Tervo, D.G.R., Proskurin, M., Manakov, M., Kabra, M., Vollmer, A., Branson, K., and Karpova, A.Y. (2014). Behavioral variability through stochastic choice and its gating by anterior cingulate cortex. *Cell* 159, 21–32.
- Tye, K.M., Prakash, R., Kim, S.-Y., Fenno, L.E., Grosenick, L., Zarabi, H., Thompson, K.R., Grardinaru, V., Ramakrishnan, C., and Deisseroth, K. (2011). Amygdala circuitry mediating reversible and bidirectional control of anxiety. *Nature* 471, 358–362.

- Valentino, R.J., and Foote, S.L. (1988). Corticotropin-releasing hormone increases tonic but not sensory-evoked activity of noradrenergic locus coeruleus neurons in unanesthetized rats. *J. Neurosci.* 8, 1016–1025.
- Valentino, R.J., and Van Bockstaele, E. (2008). Convergent regulation of locus coeruleus activity as an adaptive response to stress. *Eur. J. Pharmacol.* 583, 194–203.
- Valentino, R.J., Page, M.E., and Curtis, A.L. (1991). Activation of noradrenergic locus coeruleus neurons by hemodynamic stress is due to local release of corticotropin-releasing factor. *Brain Res.* 555, 25–34.
- Van Bockstaele, E.J., Chan, J., and Pickel, V.M. (1996). Input from central nucleus of the amygdala efferents to pericoerulear dendrites, some of which contain tyrosine hydroxylase immunoreactivity. *J. Neurosci. Res.* 45, 289–302.
- Van Bockstaele, E.J., Colago, E.E., and Valentino, R.J. (1998). Amygdaloid corticotropin-releasing factor targets locus coeruleus dendrites: substrate for the co-ordination of emotional and cognitive limbs of the stress response. *J. Neuroendocrinol.* 10, 743–757.
- Vazey, E.M., and Aston-Jones, G. (2014). Designer receptor manipulations reveal a role of the locus coeruleus noradrenergic system in isoflurane general anesthesia. *Proc. Natl. Acad. Sci. USA* 111, 3859–3864.
- Veinante, P., and Freund-Mercier, M.-J. (1998). Intrinsic and extrinsic connections of the rat central extended amygdala: an in vivo electrophysiological study of the central amygdaloid nucleus. *Brain Res.* 794, 188–198.
- Wu, Z., Autry, A.E., Bergan, J.F., Watabe-Uchida, M., and Dulac, C.G. (2014). Galanin neurons in the medial preoptic area govern parental behaviour. *Nature* 509, 325–330.